

# DEPLOYMENT OF INDOOR LTE SMALL CELLS IN TV WHITE SPACES

by

Abdelrahman Abdelkader

Directed by

Jordi Perez-Romero

Submitted in partial fulfillment of the  
requirements for the degree of  
European Master of Research on Information Technology

at

Universitat Politecnica de Catalunya BarcelonaTech (UPC)  
Barcelona, Spain  
July 2015

© Copyright by Abdelrahman Abdelkader, 2015

# Contents

<b>List of Figures</b> . . . . .	<b>vi</b>
<b>Abstract</b> . . . . .	<b>vii</b>
<b>Acknowledgements</b> . . . . .	<b>ix</b>
<b>Chapter 1 Introduction</b> . . . . .	<b>1</b>
1.1 Problem Definition . . . . .	1
1.2 Scope and Goal of this thesis . . . . .	3
1.3 Structure of this Thesis . . . . .	4
<b>Chapter 2 Literature Review</b> . . . . .	<b>5</b>
2.1 Use of TVWS to Support LTE Operation . . . . .	5
2.2 Indoor Network Planing . . . . .	8
2.2.1 Introduction . . . . .	8
2.2.2 Indoor Planning for Small Cells . . . . .	9
<b>Chapter 3 Methodology</b> . . . . .	<b>13</b>
3.1 Assumptions . . . . .	13
3.1.1 Scenario . . . . .	13
3.1.2 Radio Environment Map Information . . . . .	15

3.2	Approach 1: Maximizing Total Transmitted Power . . . . .	21
3.2.1	Optimization Problem Introduced . . . . .	21
3.2.2	Proposed Algorithm . . . . .	24
3.2.3	Perturbation Method . . . . .	28
3.3	Approach 2: Optimizing Performance Based on SINR . . . . .	29
3.3.1	Optimization Problem Introduced . . . . .	29
3.3.2	Interference Generated by DVB-T Transmitters . . . . .	31
3.3.3	Problem Solution . . . . .	32
<b>Chapter 4</b>	<b>Results . . . . .</b>	<b>33</b>
4.1	Approach 1 Results . . . . .	33
4.1.1	Original Algorithm . . . . .	33
4.1.2	Perturbation Method . . . . .	34
4.1.3	Effect of the approach on average SINR . . . . .	40
4.1.4	Exhaustive Enumeration . . . . .	42
4.2	Approach 2 Results . . . . .	44
<b>Chapter 5</b>	<b>Conclusions and suggestions for future works . . . . .</b>	<b>47</b>
5.1	Suggestions for Future Works . . . . .	48
<b>Bibliography</b>	<b>. . . . .</b>	<b>49</b>

# List of Figures

Figure 1.1	Typical scenario for HetNets [1] . . . . .	2
Figure 2.1	IMT spectrum requirements forecast [9] . . . . .	6
Figure 2.2	Typical usage of UHF TV spectrum in a specific location [11]	7
Figure 2.3	Different scenarios of CR in LTE networks [9] . . . . .	8
Figure 2.4	Scenario Plan in 2D and 3D [15] . . . . .	10
Figure 3.1	Position of DVB-T tower and measured building [4] . . . . .	14
Figure 3.2	First floor measurement points in the building and the coordinate axis [4] . . . . .	15
Figure 3.3	Measurement points located inside the building with their coordinates in meter, office location and index. Index is used to reference different points throughout this thesis . . . . .	16
Figure 3.4	3D plot of the measurement points inside our building . . . . .	18
Figure 3.5	First floor measurement points in the building [4] . . . . .	19
Figure 3.6	Flow chart of the recursive algorithm used in our first approach	25
Figure 3.7	Illustration of how the algorithm works . . . . .	27
Figure 3.8	Illustration of how the algorithm works using the perturbation method . . . . .	28

Figure 3.9	FCC DVB-T Out Of Band Emissions (OOBE) [31] . . . . .	32
Figure 4.1	Results of the proposed algorithm with $K = 2$ for different initial points. Column 1: initial position used in the algorithm, column 2,3: optimal transmitter positions for transmitter 1 and 2 for maximum total transmit power, columns 4,5: maximum transmit power for transmitter 1 and 2 in dBm, columns 6: total transmit power from both transmitters in dBm. . . . .	34
Figure 4.2	Power profile with two transmitters located at points D4-005-B and D4-111-B with acceptable power combinations in green and rejected power combinations in red, the arrows represent the result of each iteration of our algorithm . . . . .	35
Figure 4.3	Power profile with two transmitters located at points D4-005-B and D4-111-B with acceptable power combinations in green and rejected power combinations in red, the values shown represent the width of the local maximum valley . . . . .	36
Figure 4.4	Power profile with two transmitters located at points D4-005-B and D4-111-B with acceptable power combinations in green and rejected power combinations in red, the arrows represent the result of each iteration of our algorithm . . . . .	36
Figure 4.5	Results of exhaustive search to examine the effects of changing the initial point on the performance of the algorithm using the perturbation method . . . . .	37
Figure 4.6	Location and powers of optimum secondary transmitters with limit of only 2 transmitters . . . . .	38
Figure 4.7	Results of the proposed algorithm with $K = 3$ for different initial points and 0.1 dB perturbation. Columns 1: initial position used in the algorithm, columns 2,4,6: optimal transmitter positions for transmitter 1, 2 and 3 for maximum total transmit power, columns 3,5,7: maximum transmit power for transmitter 1, 2 and 3 in dBm, column 8: total transmit power in dBm. . . . .	39

Figure 4.8	Results of the proposed algorithm with $K = 3$ for different initial points and 0.2 dB perturbation. Column 1: initial position used in the algorithm, columns 2,4,6: optimal transmitter positions for transmitter 1, 2 and 3 for maximum total transmit power, columns 3,5,7: maximum transmit power for transmitter 1, 2 and 3 in dBm, column 8: total transmit power in dBm. . . .	39
Figure 4.9	Location and powers of optimum secondary transmitters with limit of only 3 transmitters . . . . .	40
Figure 4.10	Location and powers of optimum secondary transmitters with limit of only 4 transmitters . . . . .	41
Figure 4.11	Location and powers of optimum secondary transmitters with limit of only 5 transmitters . . . . .	41
Figure 4.12	A graph showing how total transmit power and SINR change with increasing number of transmitters . . . . .	42
Figure 4.13	Results of exhaustive enumeration (brute force) method . . . .	43
Figure 4.14	A table showing different min SINR required for different modulation schemes [30] . . . . .	45
Figure 4.15	A table showing results of maximizing the percentage of positions above a certain SINR threshold for different modulation schemes and their minimum SINR requirements . . . . .	45
Figure 4.16	Positions of 2 secondary transmitters placed at index 5 and index 75 in fulfillment of high SINR requirements . . . . .	46

## Abstract

This work focuses on the deployment of indoor LTE small cells acting as secondary transmitters in TVWS. Proposed methods make use of measurements stored in a Radio Environment Map (REM) that characterizes the DVB-T reception inside the building under consideration. Under this framework, this work analyses two different approaches for the deployment of small cells. First approach is based on maximizing total secondary transmit power inside the building, while the second approach is based on maximizing the percentage of positions having a Signal to Interference and Noise Ratio (SINR) above a desired threshold.

Approaches are validated by means of rigorous simulations supported by real measurements of DVB-T signal reception. Results include optimum secondary transmitter placement, and transmit power values for providing indoor LTE coverage considering operating in a channel adjacent to the one used by DVB-T. These results are compared against exhaustive enumeration techniques and proven to provide very accurate results. Results reveal that when considering system capacity or network throughput, the second approach is more efficient and provides better results than the first approach. To the author's best knowledge, this model is the only model that provides an actual deployment strategy of indoor LTE secondary transmitters while considering interference constraints from adjacent channel DVB-T transmission. While our approaches are only tested in the considered building, the methods used are generic and can be applied in the same manner within any indoor environment provided that the REM for that environment is established.

## **Keywords**

LTE, indoor deployment, small cells, TVWS, REM



## Acknowledgements

Foremost, i would like to express my sincere gratitude to my thesis director and supervisor Dr. Jordi Perez-Romero for his continuous support during my master thesis, for his patience, guidance and enthusiasm. I couldn't have done this without his support. I appreciate the time he has taken to review my work, give critical comments and discuss with me when i am confused.

Furthermore, i would like to thank my parents for their support throughout my life and for inspiring me everyday to be a better man.

# Chapter 1

## Introduction

### 1.1 Problem Definition

Demand for mobile broadband services has exponentially increased over the past years. This demand is a result of the social integration of wireless devices (smart-phones, tablets, etc.) in our every day life introducing applications that use an immense amount of bandwidth. This phenomena is expected to keep exponentially increasing in the near future due to new services being more and more used over the data network such as High Definition Video, 3 Dimensional Video, virtual reality, etc. Most of these services' traffic is generated indoors, which dictates a needed increase in link budget to provide higher data rates and satisfactory user experience. Therefore, a change in traditional network planning had to be made to provide these services with the high capacity they need. This change was achieved by the shift towards the so-called Heterogeneous Networks (HetNets). Having a mix of the traditional large macro cells as well as small cells (micro cells, pico cells, femto cells, etc.). These small cells cover small areas such as offices, rooms, hallways, etc. providing high capacity rates needed for different wireless services as well as helping remove some of the load off the large macro cells in densely populated areas. Fig.1.1 shows a typical Het-Net scenario where Macro and small cells work together to provide the best coverage possible for both outdoor and indoor environments.

The use of these HetNets will without a doubt introduce significant interference for

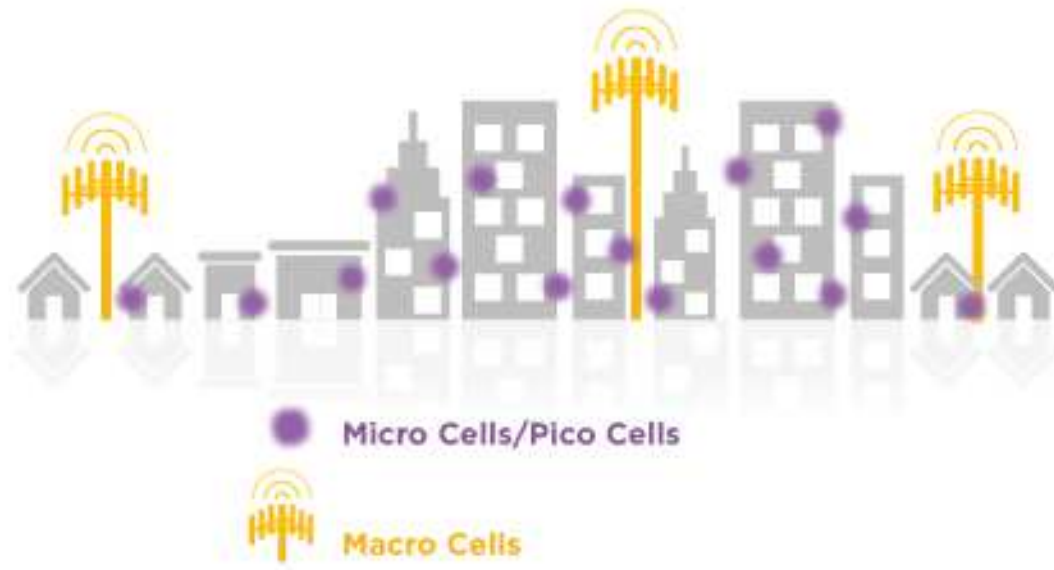


Figure 1.1: Typical scenario for HetNets [1]

both small cells affecting macro cells and vice versa will. This interference will require efficient interference mitigation techniques in case of the small cell and the macro cell sharing the same band. However, another possibility presents itself in the form of shared usage of licensed frequency bands such as TeleVision White Spaces. Different works in literature have proven the potential and feasibility of utilizing TVWS in small cell scenarios, especially for supporting LTE services. However, the design process of HetNets operating in the TV White Spaces(TVWS) is very complicated. The interference introduced by LTE services has to be small enough not to disrupt the DVB-T services operating on the co or adjacent channels.

Design and implementation of HetNets have become a research focus in the last few years. Optimal transmitter placement is considered an issue in HetNet design. The question of how to place the fewest number of transmitters to ensure the required coverage ratio while maximizing average received power and capacity of indoor areas is indeed a difficult one. First, the optimization of transmitter location is a very computationally intense operation. Second, when coupled with the transmit power

optimization the problem becomes even more complex having to optimize 2 different variables simultaneously. Third, the number of transmitters has to be minimized as well. This introduces even a third variable to our optimization problem. The condition of acceptable interference levels not to affect the DVB-T services has to be considered as well making our optimization problem even more complex.

Previously, transmitter placement used to be performed using human experience alongside trial and error. Nowadays, many computer-aided algorithms have been developed to facilitate this process using indoor propagation models and different optimization algorithms. However, most of these algorithms are only capable of optimizing either transmitter locations or the needed number of transmitters but not both simultaneously.

## 1.2 Scope and Goal of this thesis

In this thesis, we present a systematic computer-based approach to solve the problem of optimum transmitter placement for indoor LTE coverage systems operating in the TVWS. Our approach is based on 2 stages. The first stage focuses on maximizing the total transmit power. This is done through an iterative algorithm based on a direct search optimization algorithms. This algorithm is able to determine the optimum locations and transmit powers of the transmitters from a total transmit power point of view. The second stage focuses on maximizing a Quality Indicator (QI) which is the percentage of positions above a desired Signal to Noise and Interference Ratio (SINR) threshold, taking into account the interference limitation on TVWS and minimizing the number of transmitters. This is done using a similar iterative method that guarantees maximizing our QI with maximum possible transmit power and fewest number of transmitters. The overall performance of our approach is examined through

rigorous simulations.

### **1.3 Structure of this Thesis**

The remainder of this thesis is organized as follows: Chapter 2 provides an overview of previous works in the area of HetNets planning and indoor coverage optimization. The methodology of our approach will be introduced in Chapter 3. The results of our simulations and experiments will be presented in Chapter 4 along with a discussion of these results. Finally Chapter 5 concludes this thesis with some conclusions and suggestions for future work.

## Chapter 2

### Literature Review

#### 2.1 Use of TVWS to Support LTE Operation

Wireless traffic volume is expected to expand in the next few years. The traffic volume generated by consumers will soon become too overwhelming for the existing networks as demonstrated in Fig.2.1. Moreover, Many of the current allocated spectrum are significantly underutilized or even unused as shown in [2,3]. These underutilized bands are what we call White Spaces (WS). One specific spectrum band that has received a great deal of attention during the past years due to its appealing propagation characteristics is the TVWS. In [2, 3] the actual amount of TVWS is evaluated in The United States and Europe respectively. Fig.2.2 shows how underutilized is the TV band in a specific location in the UK with less than 50% utilization. Tremendous effort was put into researching possible ways to salvage and reuse this WS to aid in the support of other services such as Long term Evolution (LTE) as seen in [4–7].

To put some of these strategies and studies into action, there is a noticeable focus on specific technologies in the wireless communications research area to facilitate that. One of such technologies is Cognitive Radio (CR). CR technology was initially proposed by Joseph Mitola in [8] as a concept of a radio capable of adapting and learning from the environment. This capability has proven useful in the area of spectrum sharing and has been used ever since to resolve the problem of increasing spectrum requirements in a world where very scarce spectrum resources exist.

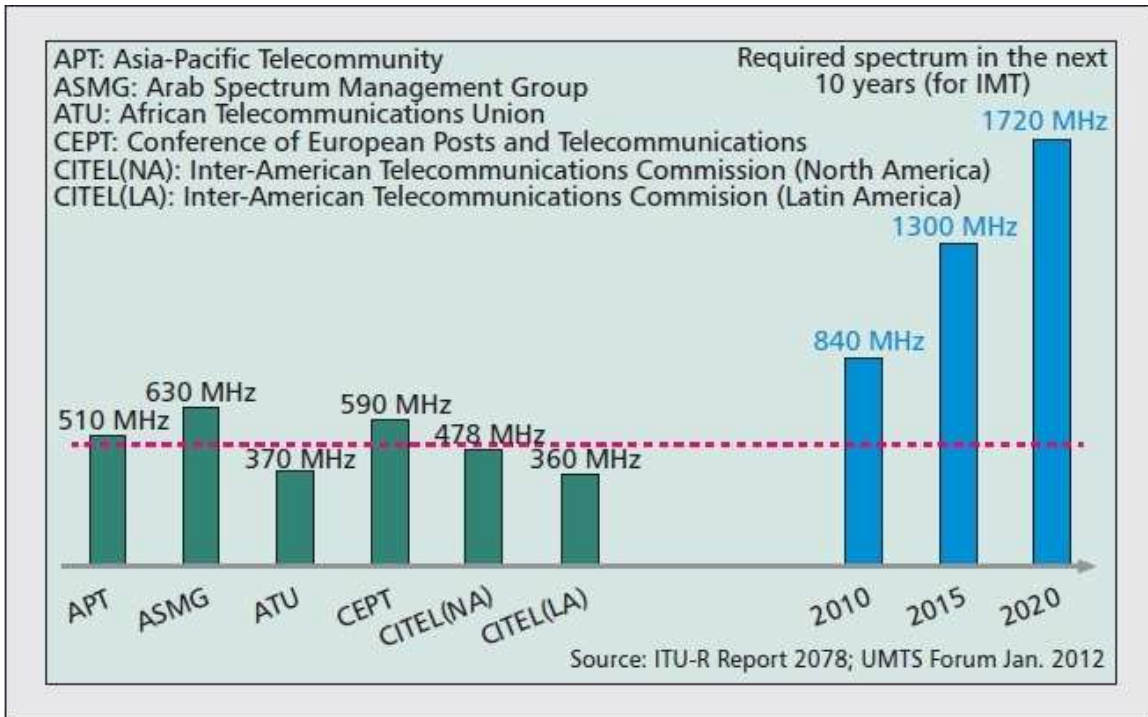


Figure 2.1: IMT spectrum requirements forecast [9]

CR technology enables Secondary Users (SU), LTE in our case, to monitor the spectrum regularly and even use it in idle periods. Once the Primary User (PU) needs the channel again, the SU switches to a different channel or terminate the communication sequence to avoid interfering with the PU. The idea here is that SUs have to be completely transparent to the PU. Meaning that the PU functions in normal operation mode without being altered or modified by the existence of a SU. Concepts such as spectrum management and spectrum sharing are explained in more details in [10].

There are many applications for CR technology. Fig.2.3 shows some operational scenarios for CR. It can be used to provide LTE over TVWS in rural or indoor areas by transmitting below a certain transmit power threshold. CR can also use TVWS for backhaul communications with the LTE core network. Using CR technology, small cells can use TVWS to avoid the co-channel interference among nearby small cells or

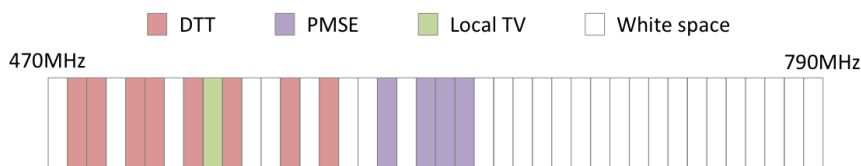


Figure 2.2: Typical usage of UHF TV spectrum in a specific location [11]

a macrocell while providing higher capacity. CR can also simply be used to provide additional spectrum for LTE services to achieve higher capacity and throughput when needed.

With these capabilities, CR can be used to allow an efficient use of locally unused TVWS. In this respect different works were carried out in the COGNITIVE radio systems for efficient sharing of TV white spaces in EUropean context (COGEU) project that aimed at taking advantage of the migration towards digital TV by developing CR systems capable of utilizing TVWS for services such as Cellular, broadband and public safety services [12]. A study was made in [13] in order to expand LTE operation into TVWS. The possibility of LTE deployment in TVWS on a larger scale was discussed in [5]. The results show that the spatial structure of the cellular network plays a greater role than expected in the secondary spectrum exploitation. So the question remains, to what extent can LTE be deployed in TVWS effectively? In [14] that question is answered. The study shows that the need to deploy new base station sites make it less appealing from a financial point of view. However, in areas where the spectrum costs are high like in India or Egypt the use of TVWS is more cost efficient for operators compared to use of licensed spectrum. An Interference study for LTE Femtocells in TVWS is presented in [15]. This study uses ray tracing method to obtain a channel profile in a typical residential building. It then demonstrates through simulations that cognitive LTE Femtocells can provide excellent indoor coverage and therefore provides a reference for future deployment of LTE Femtocells in



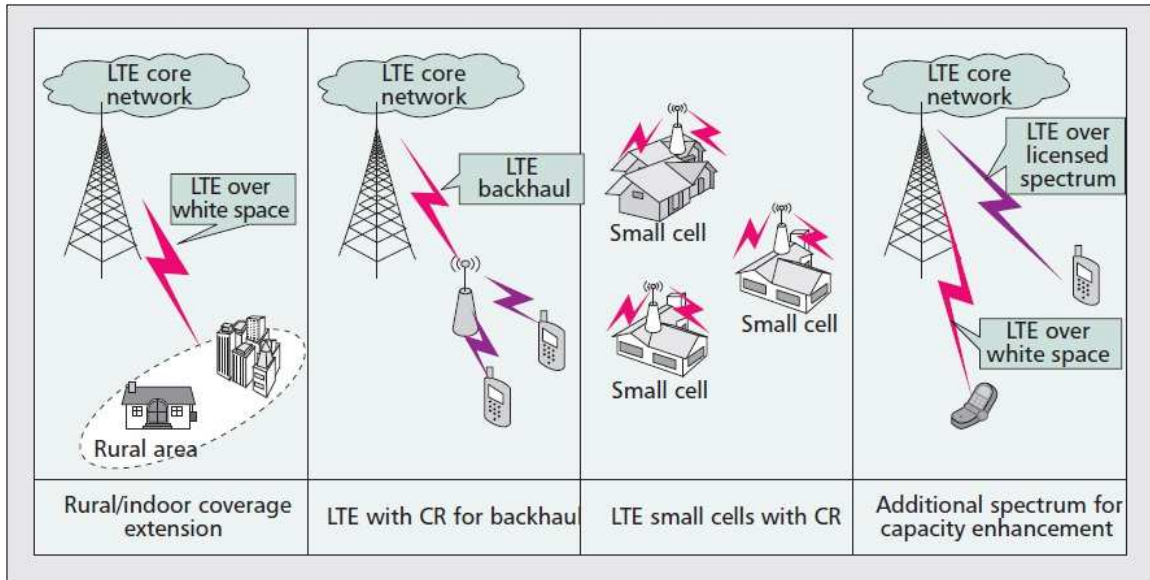


Figure 2.3: Different scenarios of CR in LTE networks [9]

TVWS. In [4, 16] a smaller scenario was considered. The study proved that indoor LTE small cells operation is possible and feasible in the Adjacent Channel (AC) to that of Digital TV. Despite proven feasible and cost efficient, almost non of the previous works in this area discussed the process of deploying LTE small cells in TVWS. That is why in this thesis will complement previous works by devising a systematic approach to deploying indoor LTE small cells in TVWS.

## 2.2 Indoor Network Planing

### 2.2.1 Introduction

Planning and optimization of cellular network resources constitutes one of the fundamental components in network design. An efficient network design through intelligent planning and optimization could have significant impacts on networks cost while increasing their supported capacities. Indoor planning and optimization in particular is of ultimate essence since it is safe to assume that the bulk of broadband traffic is

generated indoors. In fact, the importance of indoor planning has only become evident after the introduction of Distributed Antenna Systems (DAS) to enhance indoor coverage. In DAS, multiple antennas are used to provide coverage within a building. This guarantees a better chance for Line of Sight (LOS) situations with the prospect of improving the received signal quality. Accordingly, clever planning and optimization in DAS invokes designing the antenna layout (i.e., number/locations of antennas as well as the corresponding feeding network) with the prospect of maximizing throughput capacity. Previously, it usually took the efforts and experience of engineers to manually manage the network planning and optimization process through site survey.

As an effective means to improve indoor broadband services, small cells has become a research focus. Unlike DAS, small cells are designed with full base station capabilities (i.e., Frequency reuse, Handover, etc.) reducing the need for backhaul communications over radio link. Besides being low cost and low power, it can provide high quality, high speed broadband services with coverage areas raging from small rooms to big halls. They not only extend the Macro-cell coverage area for indoor scenarios but they also can achieve higher data rates. However, since the distances between the small cells are short, the interference is relatively strong. As a result, the optimization requirements for indoor small cell scenarios are much more complicated than those of outdoor environments.

### **2.2.2 Indoor Planning for Small Cells**

Over the past few years there has been a significant number of tools developed for indoor small cells planning and optimization based on analytical and numerical approaches. While analytical approaches are simpler and faster than numerical approaches, they imply a great deal of complex analysis when an optimization has to

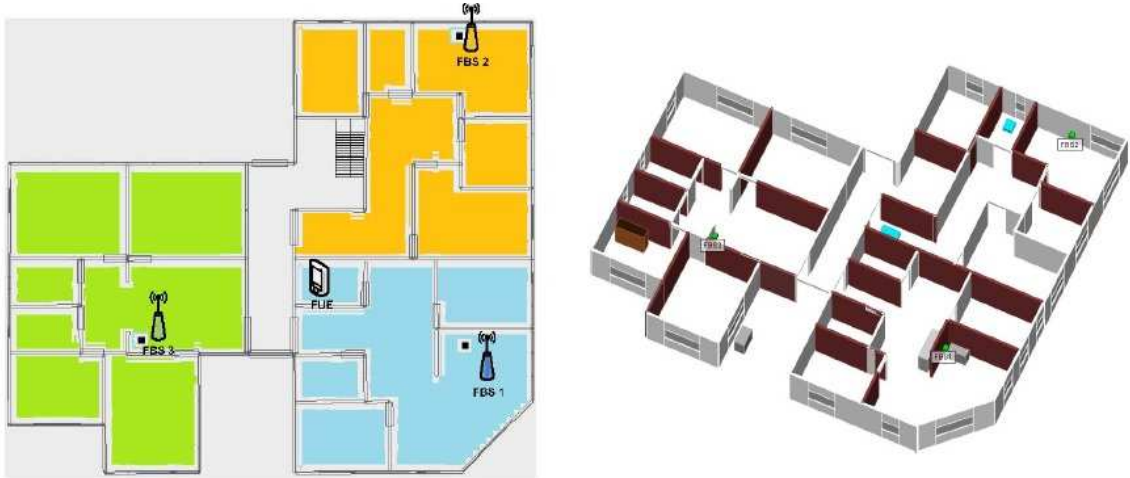


Figure 2.4: Scenario Plan in 2D and 3D [15]

be performed. One of many popular approaches is using the simplex optimization algorithm to optimally place transmitters in a given floor. In [17] a transmitter placement method is presented based on a hierarchical simplex search algorithm. Using this approach near optimal transmitter placement is guaranteed. However, like many others, this algorithm only optimizes the number and locations of transmitters, lacking therefore the ability to optimize transmit powers of previously placed transmitters.

As most of indoor planning tools, this algorithm considers every floor separately during the optimization process. As seen in Fig.2.4 floor plans are used in the simulation and not entire building plans, which in turn results in a significant loss of resources since a user can receive coverage from another floor with more efficient planning measures.

Indoor planning and optimization, as explained before, is a multi-objective optimization problem. One way of solving multi-objective optimization problems is using Genetic Algorithms (GA). A genetic algorithm starts with a population of all feasible locations. A one dimensional objective function is then used as an indicator of the fitness of every individual in the population. Multiple individuals are then

stochastically selected based on their fitness to form the new population. When the algorithm terminates due to maximum number of iterations it theoretically does not guarantee optimum solutions. A solution for indoor coverage optimization with GAs is presented in [18, 19].

In [20] a comparative study between two different optimization techniques (Kriging and GA) for optimal transmitter location in indoor environments is presented. This study showed that Kriging is an efficient tool for solving indoor optimization problems limited to the position of a single transmitter. This approach was indeed later extended for several transmitters in [21] using Transmission Line Matrix (TLM). TLM is a well-established method for wave propagation simulation. The advantage TLM presents is that it takes into account all the interactions between waves and furniture, structures and building plan. Due to the complexity of the transmitter's environment, TLM is first used to provide an accurate propagation model of the channel. This model makes it clear where it would be most beneficial to add a secondary transmitter. The combination of Kriging and TLM provides an automatic planning tool for the optimization of multiple transmitter locations in indoor environments.

A more advanced adaptive indoor optimization algorithm is presented in [22]. The Adaptive Distributed Femtocell Coverage Optimization (ADFCO) algorithm is used in LTE indoor enterprise environments. The ADFCO algorithm updates the transmitter power of femtocells depending on the users. Therefore, reducing unwanted handovers and decreases coverage gaps and overlaps. Numerical results shows 50% enhancement of overall capacity when compared to fixed transmitter power allocation techniques. Being the opposite of the previous algorithms, the ADFCO optimizes the power of transmitters but it has no way of optimizing the locations of the transmitters which has to be done manually through network planning experience.

While some of these works are very efficient in solving the indoor optimization problem in normal and even challenging indoor environments, none has considered utilizing the TVWS. Motivated by the lack of studies focusing on indoor planning considering TVWS requirements, in this paper, we propose a systematic approach to deploy LTE small cells in indoor environments while utilizing TVWS to support LTE services. This approach is an automatic tool that solves a very complex multi-objective optimization problem combining locations, powers and number of transmitters. This aids in the lowering of the traffic load on the Macro-cells and provides higher data rates indoors. This algorithm is very mathematically simple yet it delivers promising results and opens the door for more research not only focusing on LTE planning but also on general indoor network planning utilizing TVWS. Moreover, This approach considers the building plan as a whole, therefore, using resources more efficiently than other algorithms that work on a floor-by-floor basis. This not only lowers power expenditure, but results as well in less interference which in turn helps maintain high SINR values leading to an increase in overall capacity.

## Chapter 3

### Methodology

#### 3.1 Assumptions

##### 3.1.1 Scenario

Measurements of the DVB-T signals were comprehensively collected in [16] for the building of the department of Signal Theory and Communications (D4) in Universitat Politècnica de Catalunya · BarcelonaTech (UPC) Campus Nord (latitude:  $41^{\circ}23'20''$  N; longitude:  $2^{\circ}6'43''$  E; altitude: 175 m). Therefore, the indoor environment was chosen to be the same building. The Position of the DVB-T transmitter and location of considered building are shown in Fig.3.1. The building consists of 3 floors and 1 basement floor. Indoor measurements of DVB-T signal for channels 26 (514 MHz), 44(658 MHz) and 61(794 MHz) were performed in the study presented in [16]. Conclusions of this study states that it is indeed feasible to construct such a map that will allow for reliable deployment of new secondary transceivers within the building and for coexistence of different systems.

As a reference for the evaluation 83 measurement points were defined within the entire building as shown in Fig.3.5. Measurements used in this work correspond to channel 61 (794 MHz). For the scope of this thesis we will consider the worst case scenario, where the positions of the DVB-T receivers are unknown. We assume that DVB-T receivers can be located at any of these points via portable USB receivers connected

to laptops. However, in other scenarios it can also be considered where the positions of the DVB-T receivers are static or in which the only DVB-T reception point is the antenna on the rooftop. For the sake of simplicity, only these measurement points will be used. However, the same methodologies can be applied if more points exist or if interpolation is used to define more measurement points, but this is left for future works.

The locations of the measurement points are shown in Fig.3.3. These locations will be referenced many times throughout the text by their index number. For example, position 83 represents the measurement point located at D4-111-B ( $X = 29$  m,  $Y = 13$  m,  $Z = 7.5$  m).

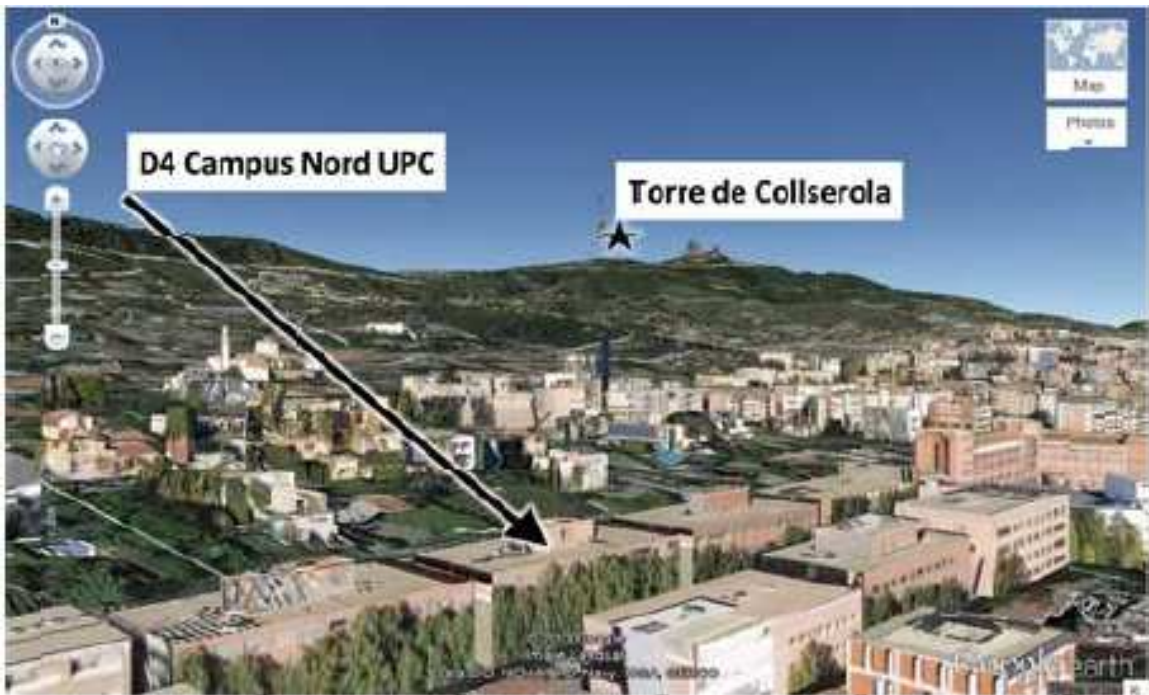


Figure 3.1: Position of DVB-T tower and measured building [4]

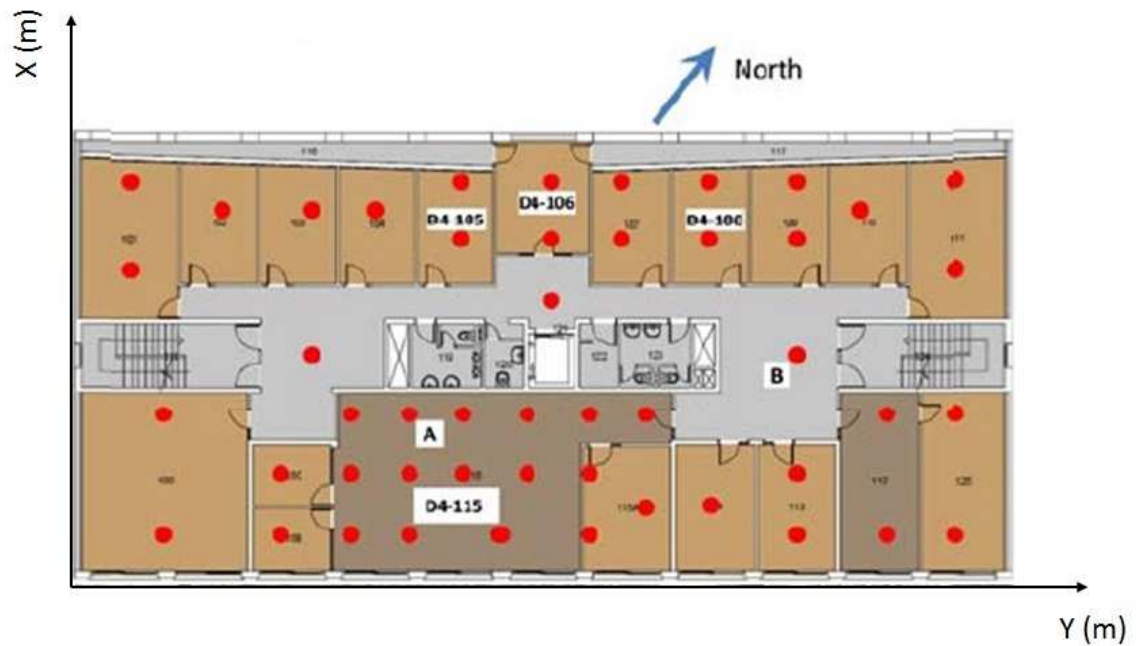


Figure 3.2: First floor measurement points in the building and the coordinate axis [4]

### 3.1.2 Radio Environment Map Information

The concept of Radio Environment Maps (REM) was first introduced by Virginia Tech scholars in [23]. REMs are centralized or distributed databases containing multi-dimensional cognitive information on the radio environment such as device locations and their activities, policies and regulations, etc. The main functionality of REMS is storage of Geo-localized measurements. The use of REMs reduces the requirement for measurements and allows for more dynamic processing of data stored such as spatial or temporal interpolation of measurements. A successful Radio Environment Map should include all information needed for deploying secondary transmitters (small cells) in the indoor environment where it applies to.

The REM database from previous works [4,16], on which this approach is based, was



Name	X	Y	Z	Index	Name	X	Y	Z	Index
D4-S110	1	3	0	1	D4-115-C1	13	3	7.5	47
D4-S109	4	3	0	2	D4-115-C2	14	1	7.5	48
D4-S108	7	3	0	3	D4-115-A3	15	5	7.5	49
D4-S107A	12	3	0	4	D4-115-C3	15	3	7.5	50
D4-S107-B	17	3	0	5	D4-115A-B2	17	1	7.5	51
D4-S107-A	22	3	0	6	D4-115A-B1	17	3	7.5	52
D4-S106	28	3	0	7	D4-115-A2	17	5	7.5	53
D4-U-D	8	7	0	8	D4-115A-B3	19	2	7.5	54
D4-U-B	16	9	0	9	D4-115-A1	19	5	7.5	55
D4-U-A	24	7	0	10	D4-114	21	2	7.5	56
D4-S102-A	11	12	0	11	D4-113-B	24	1	7.5	57
D4-S102-B	15	12	0	12	D4-113-A	24	3	7.5	58
D4-S102A	20	12	0	13	D4-112-B	27	1	7.5	59
D4-S105	28	12	0	14	D4-112-A	27	5	7.5	60
D4-016	1	3	3.3	15	D4-125-B	29	1	7.5	61
D4-015	4	3	3.3	16	D4-125-A	29	5	7.5	62
D4-014	7	3	3.3	17	D4-1F-D	8	7	7.5	63
D4-012-B	11	1	3.3	18	D4-1F-B	16	9	7.5	64
D4-012-A	11	5	3.3	19	D4-1F-A	24	7	7.5	65
D4-010-A	17	5	3.3	20	D4-101-A	2	10	7.5	66
D4-010-B	18	1	3.3	21	D4-101-B	2	13	7.5	67
D4-009	21	3	3.3	22	D4-102	5	12	7.5	68
D4-008	24	3	3.3	23	D4-103	8	12	7.5	69
D4-007	27	3	3.3	24	D4-104	10	12	7.5	70
D4-006-A	29	1	3.3	25	D4-105-A	13	11	7.5	71
D4-006-B	29	5	3.3	26	D4-105-B	13	13	7.5	72
D4-G-D	8	7	3.3	27	D4-106-A	16	11	7.5	73
D4-G-B	16	9	3.3	28	D4-106-B	16	13	7.5	74
D4-G-A	24	7	3.3	29	D4-107-A	18	11	7.5	75
D4-001-B	1	12	3.3	30	D4-107-B	18	13	7.5	76
D4-001-A	5	12	3.3	31	D4-108-A	21	11	7.5	77
D4-002	10	12	3.3	32	D4-108-B	21	13	7.5	78
D4-004	21	12	3.3	33	D4-109-A	24	11	7.5	79
D4-005-A	28	10	3.3	34	D4-109-B	24	13	7.5	80
D4-005-B	28	13	3.3	35	D4-110	26	12	7.5	81
D4-100-B	3	1	7.5	36	D4-111-A	29	10	7.5	82
D4-100-A	3	5	7.5	37	D4-111-B	29	13	7.5	83
D4-115B-F	7	1	7.5	38					
D4-115C-E	7	3	7.5	39					
D4-115-D2	9	1	7.5	40					
D4-115-D1	9	3	7.5	41					
D4-115-A6	9	5	7.5	42					
D4-115-A5	11	5	7.5	43					
D4-115-D3	11	1	7.5	44					
D4-115-D4	11	3	7.5	45					
D4-115-A4	13	5	7.5	46					

Figure 3.3: Measurement points located inside the building with their coordinates in meter, office location and index. Index is used to reference different points throughout this thesis

generated and stored using Microsoft Excel sheets. While being conveniently simple, it lacked the functionality needed to tackle complex multi-objective optimization problems which require rigorous simulations and a high level of automation. Therefore, it was essential to integrate this data using a tool such as Matlab. Some of this data is:

- $R(\theta, \theta')$ : Separation in meters between any two points of the building. Where the coordinates for one position are denoted as  $\theta = (x, y, z)$
- $L(R, n)$ : Indoor propagation model to characterise the losses between any two points of the building as a function of the separation  $R$  and building characteristics (e.g. number of floors, etc.).
- $P_r(\theta, N)$ : Received power level of the DVB-T signal at each position  $\theta$  inside the building .

A 3D plot of the measurement points inside our building is shown in Fig.3.4. This was possible to produce after loading all the data needed from the Excel sheets into matlab. Other needed data was generated using mathematical models that will be explained later on. Having all the required data in Matlab makes it possible to perform complex simulations and use more advanced optimization algorithms.

Now we turn our attention to some of our REM's content. This REM describes some of the parameters in our scenarios such as power limitations, interference and indoor propagation model. We will discuss each of these parameters in the following sections.

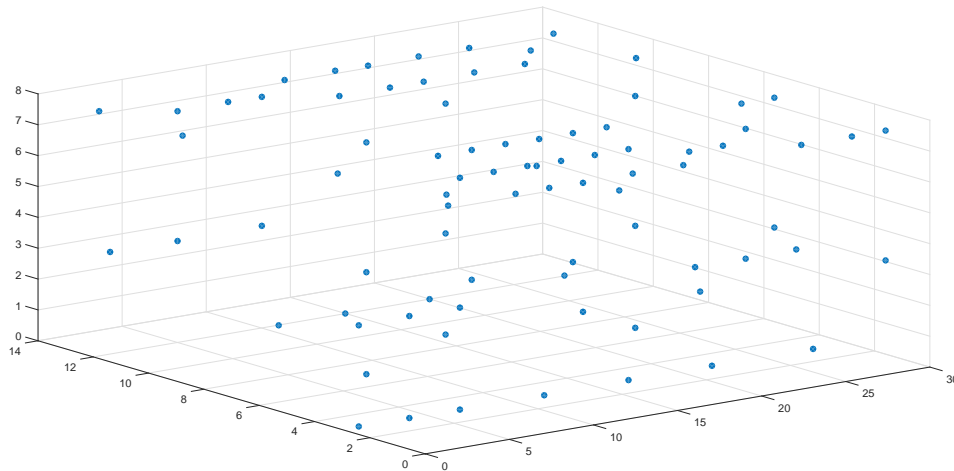


Figure 3.4: 3D plot of the measurement points inside our building

### Protection Ratio (PR)

One of the important pieces of information in our REM is the power limitation that results from the condition that the interference generated by secondary transmitters to any DVB-T receiver should be below a certain threshold not to degrade the TV reception. Requirements for successful DVB-T reception have been defined in literature [24–26]. These requirements are usually expressed in terms of the so-called Protection Ratio (PR). PR is defined as the minimum required ratio between the DVB-T signal received and the interference at a certain point, meaning that it should be satisfied that

$$\frac{P_R}{I} \geq PR \quad (3.1)$$

Where  $P_R$  is the received DVB-T signal and  $I$  is the total interference. It is important to note that PR depends on several factors. For instance, whether the DVB-T signal and the secondary transmitter are operating in the same channel and thus generate co-channel interference or in adjacent channels. In the case of adjacent channels the PR depends strongly on the selectivity of the DVB-T receiver and on the Adjacent

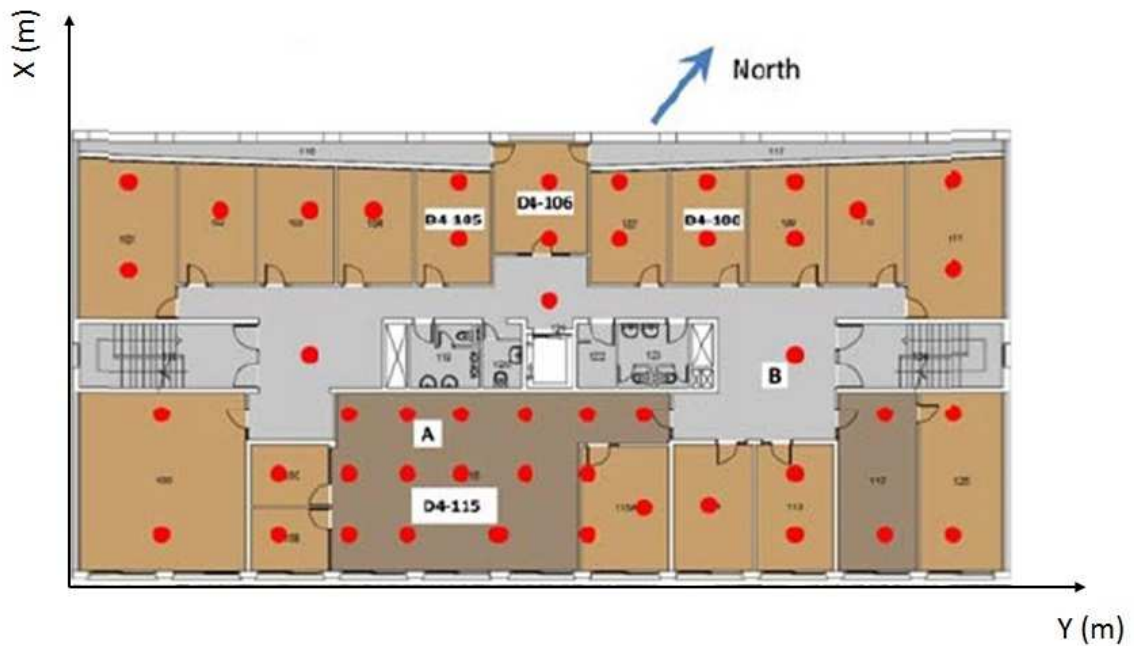


Figure 3.5: First floor measurement points in the building [4]

Channel Leakage Ratio (ACLR) of the secondary transmitter (being LTE in our case) which determines how much power exactly are leaked to adjacent channels. For the scope of this work we take as a reference a fixed PR value of -31 dB. This value was determined based on extensive measurements done in [26] for different types of DVB-T receivers and LTE transmitters while assuming LTE transmission in the first adjacent channel. This value, for the sake of future work, can be adjusted depending on the type of hardware used and in no way limits the operation of this approach.

One more thing that has to be taken into consideration is that results obtained in [4] reveal that in the considered building small cell deployment using co-channel transmission is not feasible due to the very low resulting allowed transmit power. Therefore, we limit our investigation in this paper to adjacent channel transmission, which was found more adequate for successful small cells deployment.

## Indoor Propagation Model

In order to estimate the received signal power from secondary LTE transmitters in different points within the considered building, an indoor propagation model has to be used. The FemtoForum model for suburban deployment of LTE is considered [27] in our scenario. It is worth mentioning that the exact propagation model of the considered building can be obtained by measurements but this is out of the scope of this thesis. The model considers the propagation between User Equipment (UE) and Home eNodeB (HeNB) in the case that UE is inside the same house as HeNB where

$$PathLoss = 38.46 + 20 \log_{10} R + 0.7d_{2D,indoor} + 18.3n^{((n+2)/(n+1)-0.46)} \quad (3.2)$$

where  $n$  is the number of penetrated floors,  $R$  and  $d_{2D,indoor}$  are the 3D and the 2D distances in meters between 2 points inside the building respectively

In Eqn.3.2, the path loss is modeled by free space loss, penetration loss due to internal walls and floors. The loss due to internal walls is modeled as a log-linear value, equal to  $0.7dB/m$ .

It is important to note that the above model, as noted in [27], is assuming frequency  $f = 2000MHz$ . Therefore, if we focus on the TVWS band, the path loss should be smaller. In that respect, the constant term of the path loss should be modified to account for the actual frequency of operation in TVWS by adjusting the term  $20 \log 4\pi f/c$  from  $f = 2000MHz$  to  $f_{TVWS} = 600MHz$  therefore, adding the constant term  $20 \log 600/2000 = -10.45dB$  to the path loss. The new expression for propagation loss then becomes:

$$PathLoss = 28.01 + 20 \log_{10} R + 0.7d_{2D,indoor} + 18.3n^{((n+2)/(n+1)-0.46)} \quad (3.3)$$

## 3.2 Approach 1: Maximizing Total Transmitted Power

### 3.2.1 Optimization Problem Introduced

In order to formulate our general optimization problem we have to start at the base of our scenario and work our way through different assumptions until we reach a solid general statement that describes our problem comprehensively.

1. *Maximum allowed transmit power when there is no other secondary transmitters in the building*

Assuming there is no other secondary transmitter in the building, the maximum allowed transmit power at any point  $\theta = (x, y, z)$  for an adjacent channel  $N + i$  has to fulfill the following condition for any point  $\theta'$  where a DVB-T receiver might be located:

$$\frac{P_r(\theta', N)}{P_{T_{max}}(\theta, N + i)/L(\theta', \theta)} \geq PR(i) \quad (3.4)$$

where  $L(\theta, \theta')$  is the path loss between point  $\theta$  where the secondary transmitter is located and point  $\theta'$  where a DVB-T receiver might be located, and  $i$  denotes the number of adjacent channel considered for operation. Fulfilling the condition 3.4 requires that the following expression be minimized:

$$P_{T_{max}}(\theta, N + i) = \min_{\theta' \text{ s.t. } P_r(\theta', N) \geq P_{r_{min}}} \left[ \frac{P_r(\theta', N) \cdot L(\theta', \theta)}{PR(i)} \right] \quad (3.5)$$

For the case  $\theta = \theta'$  which suggests that the secondary transmitter and the DVB-T receiver are located in the same position, we assume that minimum physical separation will always exist between the two [28], so  $L(\theta', \theta)$  equals a minimum propagation loss  $L_{min}$  which depends on the physical separation. Typical values for  $PR(i)$  are low enough in the case of adjacent channel  $N + i$  that even allow secondary transmission at a point where DVB-T reception in channel  $N$  is possible.

2. *Maximum allowed transmit power when there is another secondary transmitter placed in the building*

Now assuming there is another secondary transmitter already deployed at position  $\theta^*$  with transmit power  $P_{T_{sec}}$ , then the maximum transmit power allowed for a new secondary transmitter located at position  $\theta$ , following the same approach as before, will be:

$$P_{T_{max}}(\theta, N + i) = \min_{\theta' \text{ s.t. } P_r(\theta', N) \geq P_{r_{min}}} \left[ L(\theta, \theta') \left( \frac{P_r(\theta', N)}{PR(i)} - \frac{P_{T_{sec}}(\theta^*, N + i)}{L(\theta^*, \theta')} \right) \right] \quad (3.6)$$

However, the transmit power computed above assumes that when the second secondary transmitter is deployed, the first secondary transmitter is not modified in any way. This does not guarantee maximum total transmit power. For that, we would need to jointly determine the maximum allowed power of both

secondary transmitters simultaneously, or equivalently, at the time of deployment of the second transmitter, we will have to recompute the power of both transmitters.

3. *Maximum allowed transmit power when there are multiple secondary transmitters placed inside the building*

Knowing now that transmit powers should be jointly optimized simultaneously, we would like to determine the maximum allowed power of each of  $K$  secondary transmitters located at positions  $\theta_{k=1,2,\dots,K}$  so that the aggregated interference generated onto a DVB-T receiver located at any position  $\theta'$  is acceptable. Equivalently, the following condition must hold at any point  $\theta'$  where a DVB-T receiver might be located:

$$\frac{P_r(\theta', N)}{\sum_{k=1}^K \frac{P_{T_k}(\theta_k, N+i)}{L(\theta', \theta_k)}} \geq PR(i) \quad \forall \theta' \text{ s.t. } P_r(\theta', N) \geq P_{r_{min}} \quad (3.7)$$

The general multi-objective optimization problem can be then defined as follows:

$$\begin{aligned} & \underset{P_{T_k}, \theta_k}{max} (P_{T_1}, P_{T_2}, \dots, P_{T_K}) \\ & \text{s.t.} \quad \frac{P_r(\theta', N)}{\sum_{k=1}^K \frac{P_{T_k}(\theta_k, N+i)}{L(\theta', \theta_k)}} \geq PR(i) \quad \forall \theta' \text{ s.t. } P_r(\theta', N) \geq P_{r_{min}} \quad (3.8) \end{aligned}$$

Where we have to find the positions and transmit powers of secondary transmitters that maximizes the secondary transmit power inside the building.



### 3.2.2 Proposed Algorithm

There are many techniques to handle multi-objective optimization problems as the one we have on hand. One possibility is to convert the multi-objective optimization to a single objective optimization by combining the different optimization objectives (i.e. secondary transmit powers in our case). In this respect, a viable solution is to consider the aggregate transmit power of secondary transmitters. In this case, our optimization problem becomes:

$$\begin{aligned}
 & \underset{P_{T_k}, \theta_k}{max} (P_{T1} + P_{T2} + \dots + P_{TK}) \\
 & \text{s.t.} \quad \frac{P_r(\theta', N)}{\sum_{k=1}^K \frac{P_{T_k}(\theta_k, N+i)}{L(\theta', \theta_k)}} \geq PR(i) \quad \forall \theta' \text{ s.t. } P_r(\theta', N) \geq P_{r_{min}} \quad (3.9)
 \end{aligned}$$

Now with Eq.3.9 we have a much simpler optimization problem than the multi-objective Eq.3.8. To solve this problem, we adapt the sectioning method, a direct search algorithm, to our need [29]. Our approach works as a direct search method. First of all, initial positions and powers are assigned to K-1 secondary transmitters. It starts by calculating the maximum possible transmit power of the Kth secondary transmitter, taking into consideration the other K-1 secondary transmitters, by solving Eqn.3.9 using initial values for the first iteration. Then in a recursive manner, it keeps calculating maximum possible transmit powers until a maximum is reached. Convergence happens when the powers and positions of secondary transmitters stop changing, which occurs after a few iterations. The general flow chart of our algorithm is shown in Fig.3.6.

There are 2 different variables being optimized in Eq. 3.9. Transmit power  $P_{T_k}$  and

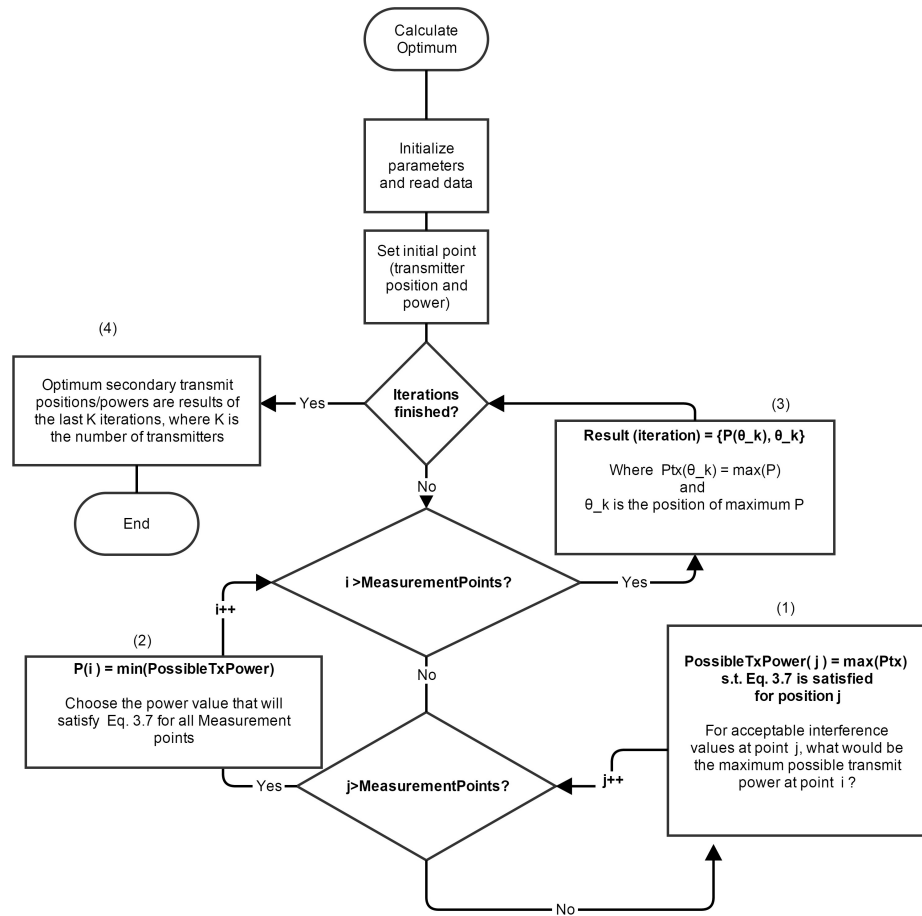


Figure 3.6: Flow chart of the recursive algorithm used in our first approach

location  $\theta_k$ . As can be seen in Fig.3.6, there are multiple loops performing different operations. First of all, choosing the initial point is very important as it affects the accuracy of the results as will be demonstrated in the results section. The innermost loop (1) computes the maximum transmit power for a secondary transmitter placed at any of the measurement points. This is done by calculating the maximum transmit power at each measurement point, denoted by its index  $i$  (representing possible  $\theta_k$ ), while still satisfying Eq. 3.7 at any DVB-T receiver position, denoted by its index  $j$  (representing  $\theta'$ ). Then, the minimum of all these possible transmitter powers is chosen in (2) because it is the transmit power that satisfies Eq. 3.7 for all positions  $j$  ( $\theta'$ ). After that, the outer loop (3) changes the transmitter position  $i$ , and repeats both operations (1) and (2) until all measurement points are checked. It then chooses the position with maximum secondary transmit power, and by doing that optimizes the position as well as the power. Finally, the algorithm does multiple iterations of the previous steps, iterating from one transmitter to another, until they all converge. Operation (4) considers only the last  $K$  iterations representing the number of transmitters considered. Since each iteration represents the optimization process of one secondary transmitter, then results of these last  $K$  iterations represent optimum positions and powers of all  $K$  secondary transmitters. The algorithm returns the optimum power and location of secondary transmitters for indoor deployment. The algorithm in Fig.3.6 is for a fixed number of transmitters  $K$ . Repeating this for different numbers of transmitters  $K$  allows us to examine the effect of  $K$  on total secondary transmit power.

While the number of secondary transmitters deployed inside the building  $K$  is present in the optimization problem, it has no sense to make it an optimization objective as an increase in the number of secondary transmitters will always constitute an increase in total secondary transmit power. Also, as will be discussed in more details in

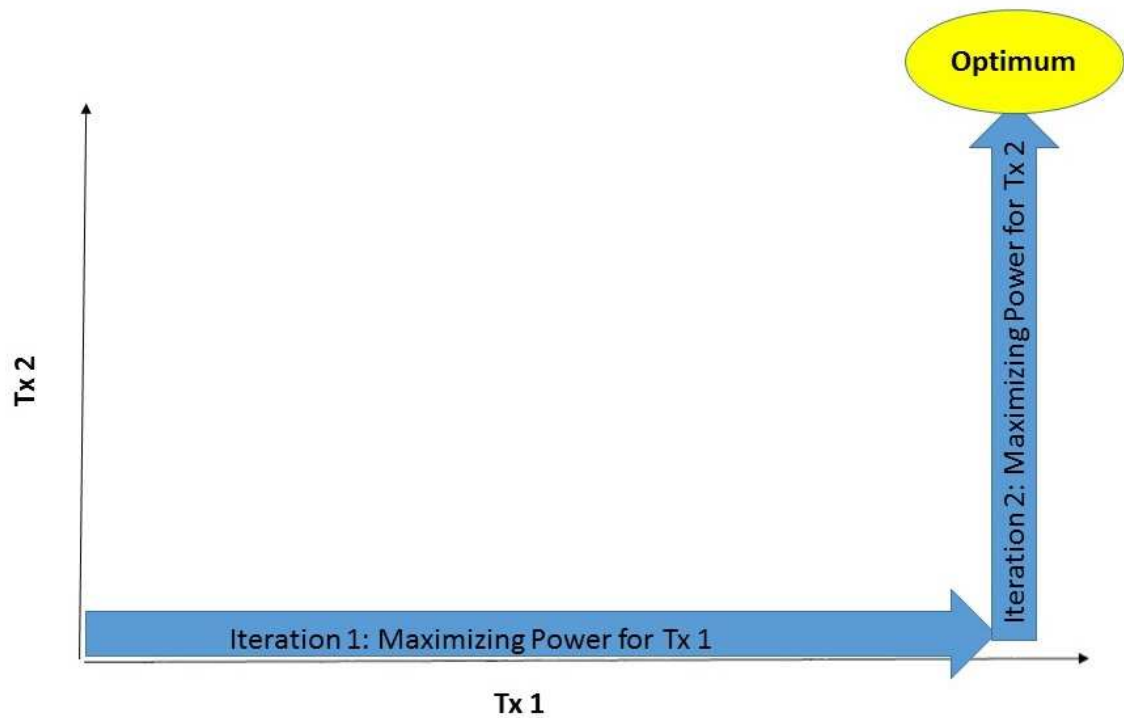


Figure 3.7: Illustration of how the algorithm works

the results section, while an increase in the number of secondary transmitters most definitely constitutes an increase in total transmit power, it is not always considered beneficial from a network throughput or capacity point of view.

To better describe the details of our approach, let us consider the case of only two secondary transmitters placed at arbitrary locations and take a look at how the algorithm operates. The basic idea of a direct search algorithm is that it operates on each axis (corresponding to one secondary transmitter in our case) separately as illustrated in Fig.3.7. The algorithm starts by maximizing the transmit power for the first transmitter, then maximizes the transmit power for the second transmitter and keeps doing that recursively until a maximum is reached.

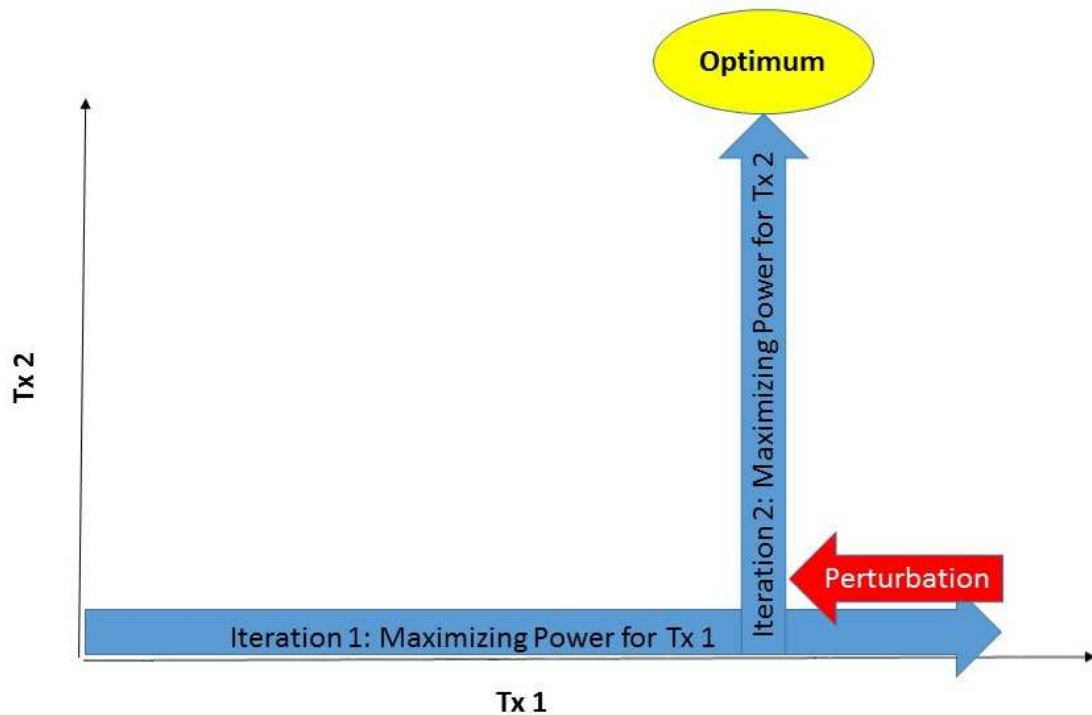


Figure 3.8: Illustration of how the algorithm works using the perturbation method

### 3.2.3 Perturbation Method

Rigorous simulations show that it is possible for the algorithm to converge on a local maximum. This will be explained in more details in the results section. This problem of local maximums calls for a modification of our original algorithm. It has been empirically found, as will be shown in the results section, that performance can be improved by introducing a slight perturbation in the resulting transmit power after each iteration. A slight decrease in the resulting transmit power of each iteration can ensure that the algorithm converges on a global maximum every time it operates. This operation is shown in Fig.3.8. The final values are checked at the end to make sure that the interference values remain in the acceptable region for all DVB-T possible receiving points. In the results section we will demonstrate why this modification leads to more accurate and consistent results.

As shown in the Figure, the subtraction of the perturbation value causes the optimization algorithm to steer the result away from any local maximums that can produce wrong results. Empirical trial and error experiments were performed to decide an optimal value for the perturbation. It was found that best results, which mean guaranteed convergence, occur at a value of 0.2 dB. This value is subtracted from the resulting power of each iteration in dBm. Lower values of the perturbation do not provide a solution for the problem of inconsistency, while higher values of the perturbation cause deviation from the global optimum which increases with the increase of this value.

### **3.3 Approach 2: Optimizing Performance Based on SINR**

#### **3.3.1 Optimization Problem Introduced**

An increase in the number or power of secondary transmitters means an increase in Inter Cell Interference (ICI) which in turn, decreases the Signal to Interference and Noise Ratio (SINR) and capacity of the network. Therefore, a second approach is suggested. Our general optimization problem so far was formulated based on maximizing transmit power of secondary transmitters. However, this leads to a decrease in the average SINR in the building leading to lower capacity values as will be explained in details in the results section. Therefore, this is not the most efficient approach. For that, we have to formulate a new optimization problem that takes more into consideration network throughput and capacity. We first define a QI representing the percentage of positions in the building above a desired SINR threshold. Then, our second approach is to maximize this QI while keeping the interference levels in all DVB-T possible receiving positions within the acceptable range. Our new optimization problem is then:

$$\begin{aligned}
& \underset{P_{T_k, \theta_k, K}}{\text{arg max}}(QI) \\
& \text{s.t.} \quad \frac{P_r(\theta', N)}{\sum_{k=1}^K \frac{P_{T_k}(\theta_k, N+i)}{L(\theta', \theta_k)}} \geq PR(i) \quad \forall \theta' \text{ s.t. } P_r(\theta', N) \geq P_{r_{min}} \quad (3.10)
\end{aligned}$$

Where QI is the percentage of positions  $\theta'$  where the following condition holds:

$$\frac{P_{T_n}(\theta_n)/L(\theta', \theta_n)}{P_{Noise} + \sum_{\substack{k=1 \\ k \neq n}}^K \frac{P_{T_k}(\theta_k, N+i)}{L(\theta', \theta_k)}} \geq SINR_{th} \quad (3.11)$$

Where Transmitter n is the transmitter providing coverage to position  $\theta'$  (i.e. the transmitter with highest received power  $P_{T_n}/L(\theta', \theta_n)$ ),  $SINR_{th}$  is the desired SINR based on modulation and encoding requirements, and the noise power measured in the channel is:

$$P_{Noise} = K \cdot t_o \cdot F \cdot B \quad (3.12)$$

Where  $B = 8 \text{ MHz}$  and  $K \cdot t_o = -174 \text{ dBm/Hz}$ , and Noise Figure (F) is assumed to be 7 dB. The noise power is then  $P_{Noise} \simeq -98 \text{ dBm}$ .

From what can be seen in Eqn.3.11, and unlike our first approach, the number of transmitters K is an important objective in our optimization problem. This optimization problem tries to maximize the introduced QI by optimizing three different

variables. The number of secondary transmitters  $K$ , the transmit power of each secondary transmitter  $P_{T_k}$  and the location of each secondary transmitter  $\theta_k$ . It is also important to note that the expression in Eqn.3.11 does not consider the interference generated by DVB-T transmitters operating in the adjacent channel. This will be explained in more detail in the next section.

### 3.3.2 Interference Generated by DVB-T Transmitters

The interference exerted from DVB-T transmitters on LTE receivers must be considered for successful LTE operations. This interference can handicap the LTE service operations, therefore has to be monitored and mitigated. It depends on the selectivity of LTE receivers and the ACLR of DVB-T transmitters. According to the following expression, where  $P_{Rx}$  is the power received by DVB-T receivers in the adjacent channel:

$$I = P_{Rx} \left( \frac{1}{\text{Selectivity}} + \frac{1}{\text{ACLR}} \right) \quad (3.13)$$

In [30] the selectivity of LTE receivers are found to be in the range of 43 dB. In [31] the ACLR of DVB-T transmitters as shown in Fig.3.9 are found to be 55 dB for adjacent channels  $N \pm 1$ . Moreover, the average DVB-T  $P_{Rx}$  was found in [16] to be ranging from -58 dBm to -78 dBm depending on the position within our indoor environment. In this respect, the interference values are in the range of -100 dBm to -120 dBm, which is lower than the noise power ( $P_{Noise} = -98\text{dBm}$ ). These values are also relatively low when compared to ICI between different small cells (i.e. different secondary transmitters) which our simulations show that it ranges between -80 dBm and -100 dBm. Therefore, in our study, it is safe to neglect the interference exerted



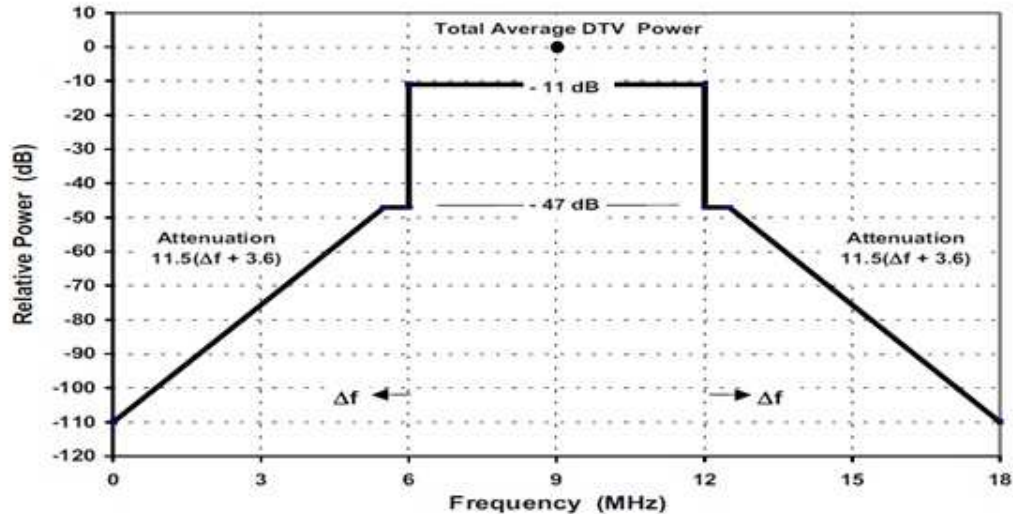


Figure 3.9: FCC DVB-T Out Of Band Emissions (OOBE) [31]

from DVB-T transmitters on LTE receivers.

### 3.3.3 Problem Solution

To solve this problem, we use the exhaustive enumeration method [32]. Despite being time consuming, exhaustive enumeration provides a way to verify if this approach is indeed more efficient than our previous approach. This method uses all possible combinations of powers and positions and calculates SINR values at all points. Then chooses the powers and locations that maximize our QI while still fulfilling the condition in Eq.3.4. For the scope of this thesis, we will only consider results generated by exhaustive enumeration. More efficient solutions are left for future works.

## Chapter 4

### Results

After introducing our approaches, it is important to see how they perform in our scenario. Several simulations have been executed to test our algorithms in many aspects such as accuracy, time consumption and network throughput.

#### 4.1 Approach 1 Results

##### 4.1.1 Original Algorithm

The proposed algorithm returns the position (represented by the index of the measurement point corresponding to it) and transmit power of secondary transmitters to achieve maximum possible total secondary transmit power. Using exhaustive search [32], it was possible to examine the effect of changing the initial point on the recursive algorithm. The algorithm is calculated 83 times with 83 different initial points with the same initial power. Results shown in Fig.4.1. These simulations show that results vary depending on the initial points used. Different locations and powers appear every time the initial point is changed which leads to inconsistent (changing with changing of initial point) and possibly unreliable (optimum is not guaranteed) algorithm output.

In order to analyze the source of this behavior, the power profile of two transmitters placed at positions D4-005-B and D4-111-B is depicted in Fig.4.2. Using all possible

Index of Initial position	Index of Tx1 Position	Index of Tx2 Position	Transmit power for Tx1	Transmit power for Tx2	Total secondary transmit power
64	83	35	8.920090861	8.180759045	11.57643869
62	80	35	8.906627937	8.183776521	11.57052402
79	80	35	8.906639518	8.182377045	11.56988871
77	80	35	8.906647843	8.181370767	11.56943197
54	80	35	8.906648012	8.181350304	11.56942268
80	80	35	8.906648012	8.181350304	11.56942268
78	80	35	8.906651053	8.180982697	11.56925584
59	80	35	8.906651095	8.180977606	11.56925353
61	80	35	8.906651095	8.180977606	11.56925353
52	80	35	8.906651338	8.18094822	11.5692402
75	80	35	8.906652094	8.180856817	11.56919871
83	80	35	8.82497119	8.193505598	11.53100517
76	83	35	8.925349194	8.072687281	11.53021034
81	80	35	8.702147511	8.193822344	11.46571783
50	83	35	8.927122685	7.896998813	11.45283188
82	80	35	8.635228345	8.193991178	11.43051095
73	83	35	8.931891993	7.385512125	11.23746835
74	83	35	8.942783863	5.922736869	10.70044987
51	83	33	8.949125934	5.691104956	10.62902476
24	83	33	8.947659991	5.6911097	10.62803064

Figure 4.1: Results of the proposed algorithm with  $K = 2$  for different initial points. Column 1: initial position used in the algorithm, column 2,3: optimal transmitter positions for transmitter 1 and 2 for maximum total transmit power, columns 4,5: maximum transmit power for transmitter 1 and 2 in dBm, columns 6: total transmit power from both transmitters in dBm.

transmit power combinations, the interference at all possible DVB-T receivers is calculated. Power combinations that satisfy the interference constraints in Eq. 3.7 are then plotted in green, and power combinations that do not fulfill these constraints are plotted in red. As you can see the power profile is very linear, except for the marked area. This marked edge is considered a local maximum. Applying the basic concept of operation explained in Fig.3.7 then it is possible to converge onto this local maximum as indicated on Fig.4.2.

#### 4.1.2 Perturbation Method

##### Considering Two secondary transmitters $K=2$

This method was introduced to the original algorithm in order to provide a solution for the above-mentioned problem of local maximums. To determine a suitable value

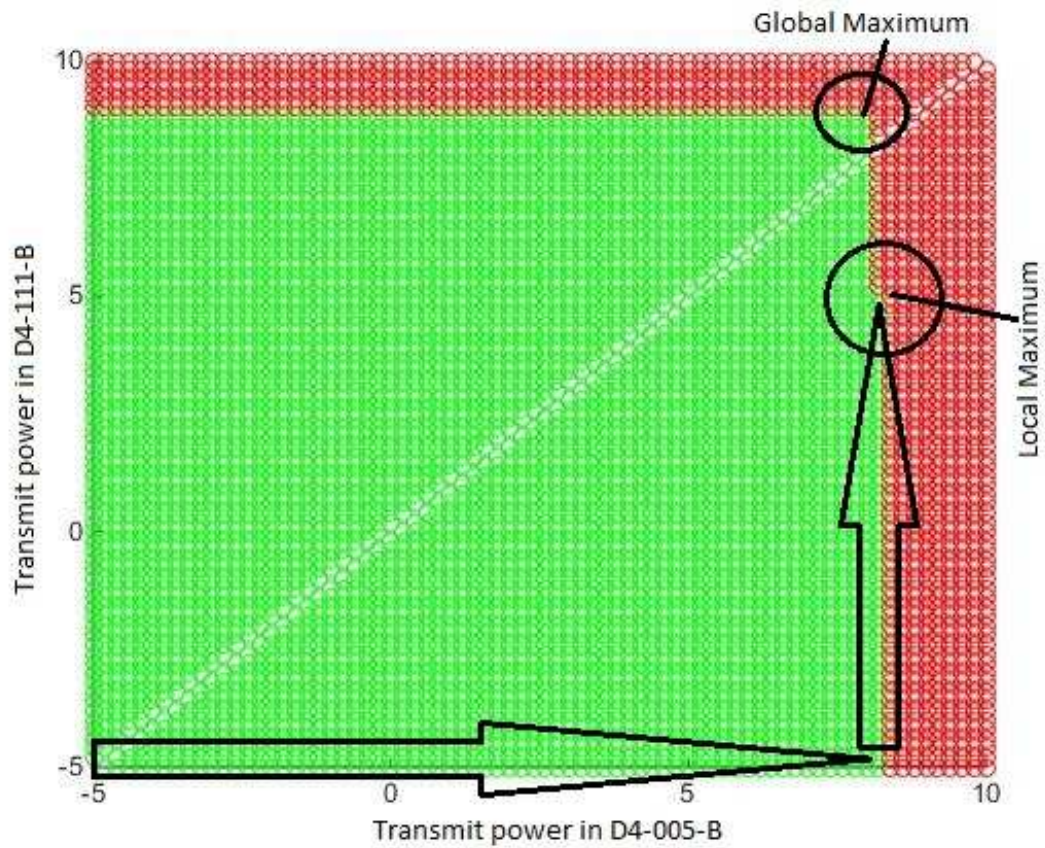


Figure 4.2: Power profile with two transmitters located at points D4-005-B and D4-111-B with acceptable power combinations in green and rejected power combinations in red, the arrows represent the result of each iteration of our algorithm

for the perturbation, many simulations were made considering fixed transmitter locations. These simulations aim at examining the local maximums in more depth. Fig.4.3 shows that the local maximum is in the range of 0.1 dB in width. However, this result is for two secondary transmitters only.

when the concept of operation depicted in Fig.3.8, explaining the perturbation method, is applied to the same power profile as before, convergence always occurs on the global optimum as explained in Fig.4.4

The same exhaustive search is repeated for the algorithm using the perturbation method and results were independent on initial points as shown in Fig.4.5. Powers

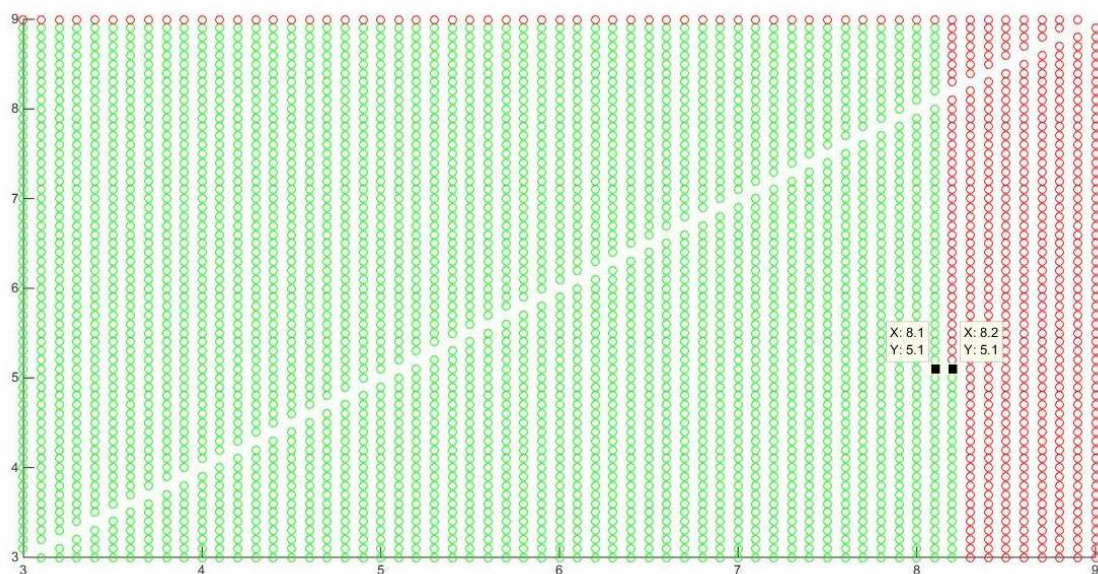


Figure 4.3: Power profile with two transmitters located at points D4-005-B and D4-111-B with acceptable power combinations in green and rejected power combinations in red, the values shown represent the width of the local maximum valley

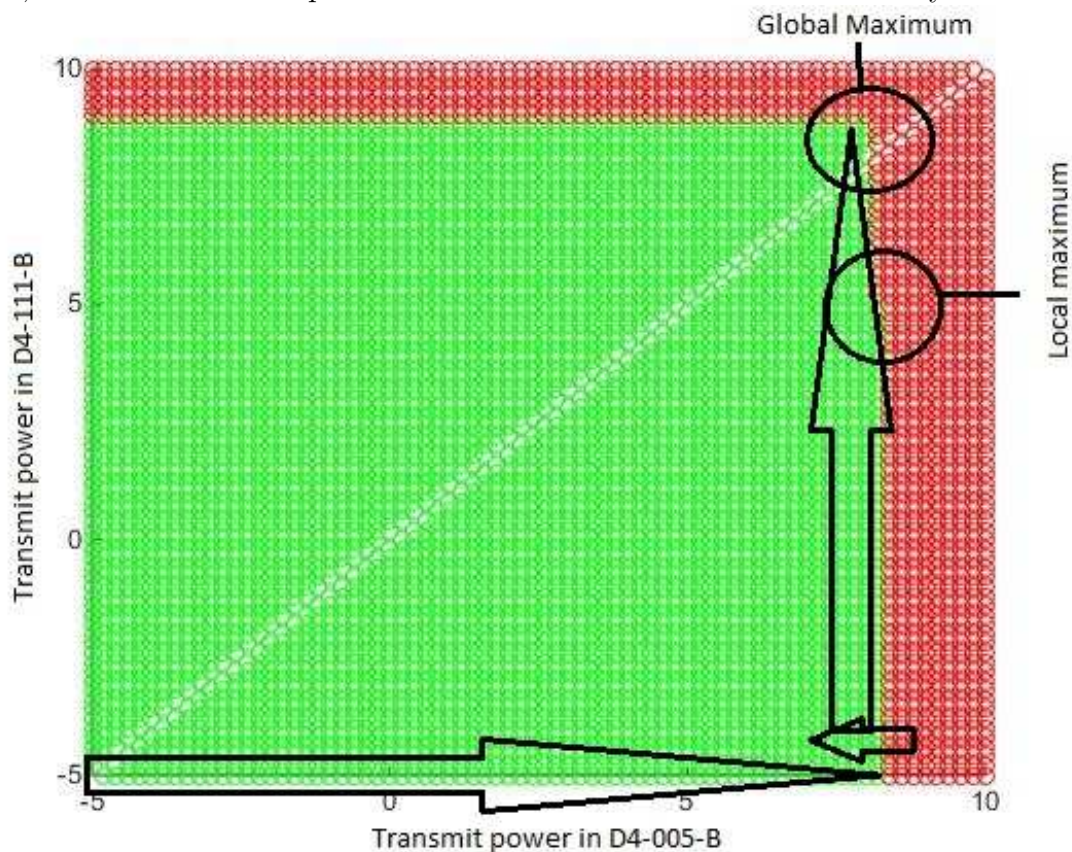


Figure 4.4: Power profile with two transmitters located at points D4-005-B and D4-111-B with acceptable power combinations in green and rejected power combinations in red, the arrows represent the result of each iteration of our algorithm

Index of initial point	Index of Tx 1 Position	Index of Tx 2 Position	Transmit power of Tx 1	Transmit power of Tx 2	Total secondary transmit power
1	83	35	8.726277918	8.18181332	11.47287227
2	83	35	8.726277918	8.18181332	11.47287227
3	83	35	8.726277918	8.18181332	11.47287227
4	83	35	8.726277918	8.18181332	11.47287227
5	83	35	8.726277917	8.18181332	11.47287227
6	83	35	8.726277914	8.18181332	11.47287227
7	83	35	8.726277909	8.18181332	11.47287227
8	83	35	8.726277918	8.18181332	11.47287227
9	83	35	8.726277918	8.18181332	11.47287227
10	83	35	8.726277913	8.18181332	11.47287227
11	83	35	8.726277918	8.18181332	11.47287227
12	83	35	8.726277918	8.18181332	11.47287227
13	83	35	8.726277917	8.18181332	11.47287227
14	83	35	8.726277916	8.18181332	11.47287227
15	83	35	8.726277918	8.18181332	11.47287227
16	83	35	8.726277917	8.18181332	11.47287227
17	83	35	8.726277917	8.18181332	11.47287227
18	83	35	8.726277914	8.18181332	11.47287227
19	83	35	8.726277914	8.18181332	11.47287227
20	83	35	8.726277894	8.18181332	11.47287226

Figure 4.5: Results of exhaustive search to examine the effects of changing the initial point on the performance of the algorithm using the perturbation method

shown in previous Fig.4.1 appear to be in some cases higher than the optimum resulting in Fig.4.5. This is expected as the algorithm reaches an answer as close as possible to an optimum in the order of 0.1 dB as shown by the difference between the highest power value in Fig.4.1 which is 11.576 dBm and the power values shown in Fig.4.5 of 11.473 dBm. This is a small sacrifice in order to make the algorithm more consistent.

Fig.4.6 shows graphically the optimum locations and transmit powers for the case of 2 transmitters. as you can see the algorithm shows the locations and gives the transmit power in dBm.

### Considering Three Secondary Transmitters $K=3$

Further analysis was performed using higher number of transmitters and values of perturbations varying around 0.1 dB. Due to dimensionality problems, it is difficult to show it graphically. However, Fig.4.7 and Fig.4.8 show results of the algorithm using the perturbation method for 3 secondary transmitters with perturbation values

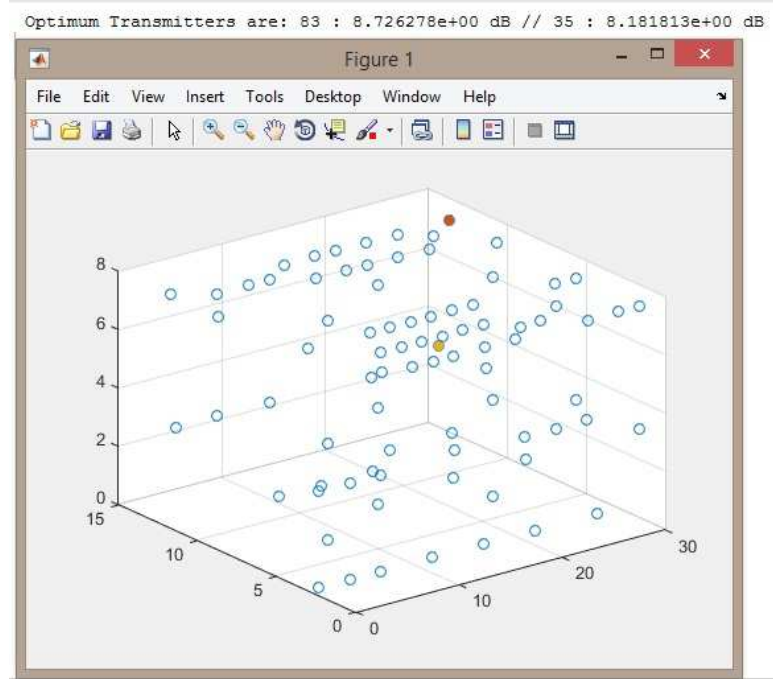


Figure 4.6: Location and powers of optimum secondary transmitters with limit of only 2 transmitters

of 0.1 dB and 0.2 dB respectively and different initial points. These simulations proved, as mentioned in section 3.2.3, that higher values than 0.2 dB of perturbation causes a much higher deviation from the optimum transmit power value, and lower values than 0.1 dB produces very inconsistent results.

Fig.4.9 shows graphically the optimum locations and transmit powers for the case of 3 transmitters. as you can see the algorithm shows the locations and gives the transmit power in dBm. The results for 4 and 5 transmitters are shown in Fig.4.10 and Fig.4.11. We observe that the transmitters are always clustered in one area (first floor, North side). This observation is explainable if we consider the location of the DVB-T transmitter. In order to provide higher secondary transmit power, the algorithm had to place the transmitters in positions with higher DVB-T received signal strength, that are closest to the DVB-T transmitter located north of the building, so that the PR constraint in Eq.3.7 stays fulfilled while increasing secondary transmit power.

Index of initial point	Index of Tx 1 position	Transmit power of Tx 1	Index of Tx 2 position	Transmit power of Tx 2	Index of Tx 3 position	Transmit power of Tx 3	Total transmit power
1	30	4.0090	83	8.8251	35	8.1809	12.2336
2	30	4.0090	35	8.0810	83	8.9252	12.2410
3	30	4.0090	35	8.0810	83	8.9252	12.2409
4	30	4.0090	35	8.0810	83	8.9252	12.2409
5	30	4.0090	35	8.0808	83	8.9252	12.2409
6	30	4.0090	35	8.0802	83	8.9252	12.2406
7	30	4.0090	35	8.0791	83	8.9252	12.2402
8	30	4.0090	35	8.0810	83	8.9252	12.2409
9	33	4.5727	35	7.3143	83	8.9192	12.0550
10	30	4.0090	35	8.0766	83	8.9252	12.2393
11	30	4.0090	35	8.0810	83	8.9252	12.2409
12	30	4.0090	35	8.0808	83	8.9252	12.2409
13	30	4.0090	35	8.0798	83	8.9252	12.2405
14	35	8.0806	30	4.0100	83	8.9252	12.2409
15	30	4.0090	35	8.0807	83	8.9252	12.2408
16	30	4.0090	35	8.0803	83	8.9252	12.2407
17	30	4.0090	35	8.0796	83	8.9252	12.2404
18	35	8.0807	30	3.4651	83	8.9252	12.1633
19	30	4.0090	35	8.0766	83	8.9252	12.2393

Figure 4.7: Results of the proposed algorithm with  $K = 3$  for different initial points and 0.1 dB perturbation. Columns 1: initial position used in the algorithm, columns 2,4,6: optimal transmitter positions for transmitter 1, 2 and 3 for maximum total transmit power, columns 3,5,7: maximum transmit power for transmitter 1, 2 and 3 in dBm, column 8: total transmit power in dBm.

Index of initial point	Index of Tx 1 position	Transmit power of Tx 1	Index of Tx 2 position	Transmit power of Tx 2	Index of Tx 3 position	Transmit power of Tx 3	Total transmit power
1	33	4.2564	35	7.7316	83	8.9163	12.1452
2	33	4.2564	35	7.7316	83	8.9163	12.1452
3	33	4.2564	35	7.7316	83	8.9163	12.1452
4	33	4.2564	35	7.7316	83	8.9163	12.1452
5	33	4.2564	35	7.7316	83	8.9163	12.1452
6	33	4.2564	35	7.7316	83	8.9163	12.1452
7	33	4.2564	35	7.7316	83	8.9163	12.1452
8	33	4.2587	35	7.7237	83	8.9164	12.1428
9	33	4.2564	35	7.7315	83	8.9163	12.1452
10	33	4.2564	35	7.7316	83	8.9163	12.1452
11	33	4.2564	35	7.7316	83	8.9163	12.1452
12	33	4.2564	35	7.7316	83	8.9163	12.1452
13	35	7.7326	33	4.2113	83	8.9164	12.1383
14	33	4.2564	35	7.7316	83	8.9163	12.1452
15	33	4.2564	35	7.7316	83	8.9163	12.1452
16	33	4.2564	35	7.7316	83	8.9163	12.1452
17	35	7.7326	33	4.2112	83	8.9164	12.1383
18	33	4.2564	35	7.7315	83	8.9163	12.1452
19	35	7.7315	33	4.2105	83	8.9164	12.1378

Figure 4.8: Results of the proposed algorithm with  $K = 3$  for different initial points and 0.2 dB perturbation. Column 1: initial position used in the algorithm, columns 2,4,6: optimal transmitter positions for transmitter 1, 2 and 3 for maximum total transmit power, columns 3,5,7: maximum transmit power for transmitter 1, 2 and 3 in dBm, column 8: total transmit power in dBm.



```
>> Expansion3Tx
Optimum Transmitters are: 33 : 4.256417e+00 dB // 35 : 7.731584e+00 dB // 83 : 8.916304e+00 dB
>>
```

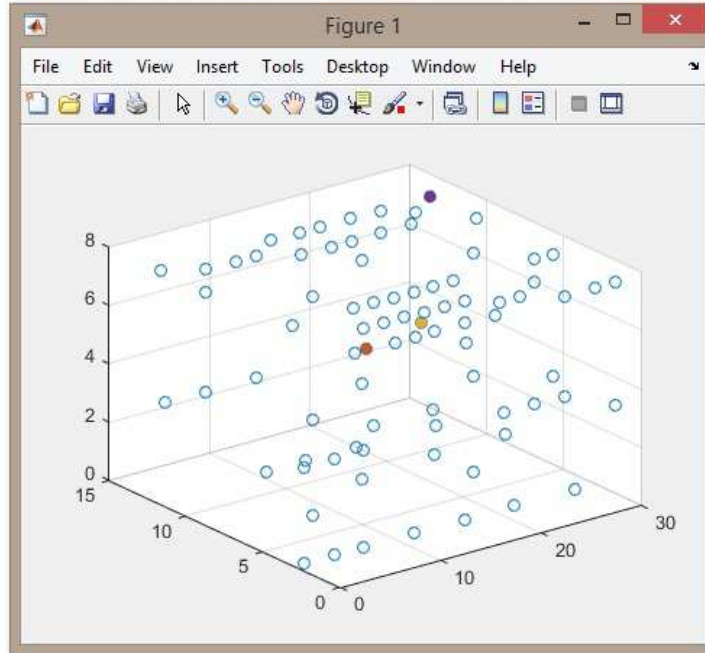


Figure 4.9: Location and powers of optimum secondary transmitters with limit of only 3 transmitters

#### 4.1.3 Effect of the approach on average SINR

In order to investigate the efficiency of our approach from a SINR point of view, total transmit power is plotted on the same curve as the average SINR against the increasing number of secondary transmitters for the cases of 2, 3, 4, and 5 transmitters. Results are shown in Fig.4.12. As can be seen, increasing the number of transmitters causes an increase in total transmit power. This, in turn, causes an increase in ICI and results in a drop in the average SINR (defined as the averaging of measured SINR between all measurement points). This drop is also emphasized by the clustering of secondary transmitters. In the case of 5 transmitters, a secondary transmitter is placed in the other side of the building away from the transmitter cluster. This positioning causes the average SINR to be higher than in the case of 4 transmitters. With these results, it is very clear that maximizing total secondary transmit power

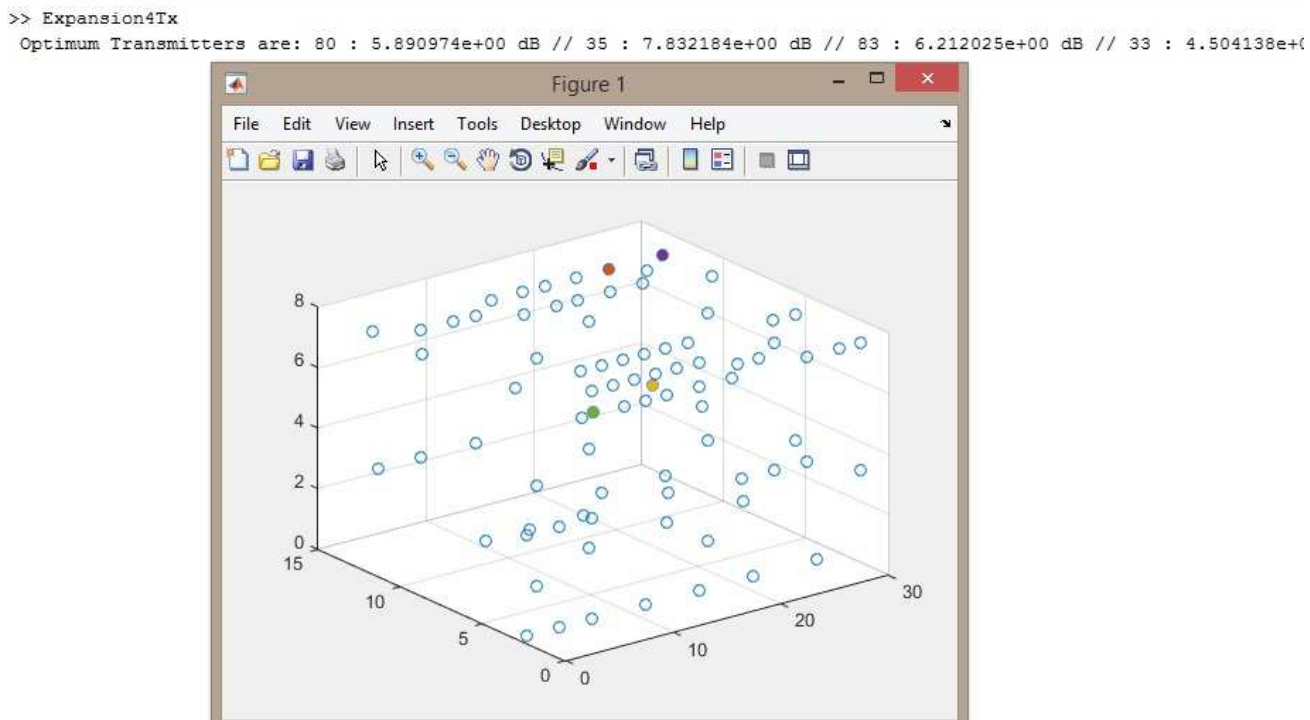


Figure 4.10: Location and powers of optimum secondary transmitters with limit of only 4 transmitters

```
>> Expansion5Tx
Optimum Transmitters are: 30 : 3.906907e+00 dB // 80 : 5.553685e+00 dB
// 83 : 6.482027e+00 dB // 33 : 4.038526e+00
// 35 : 8.040589e+00 dB
```

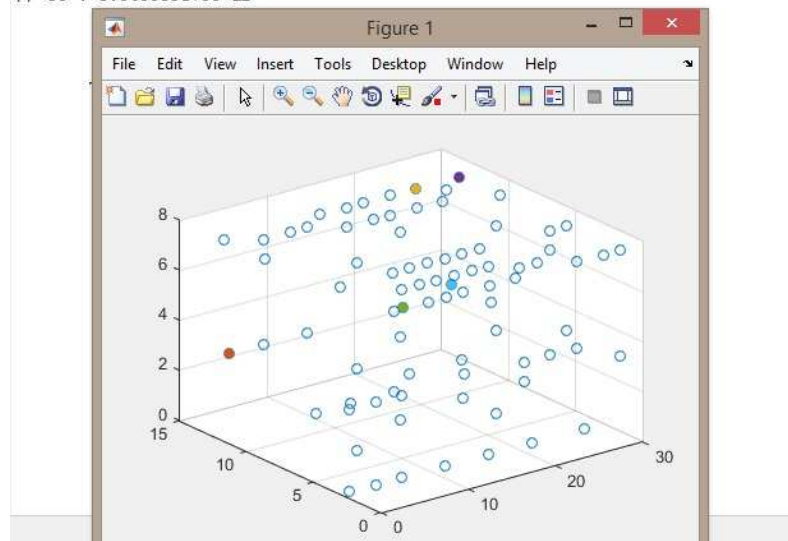


Figure 4.11: Location and powers of optimum secondary transmitters with limit of only 5 transmitters

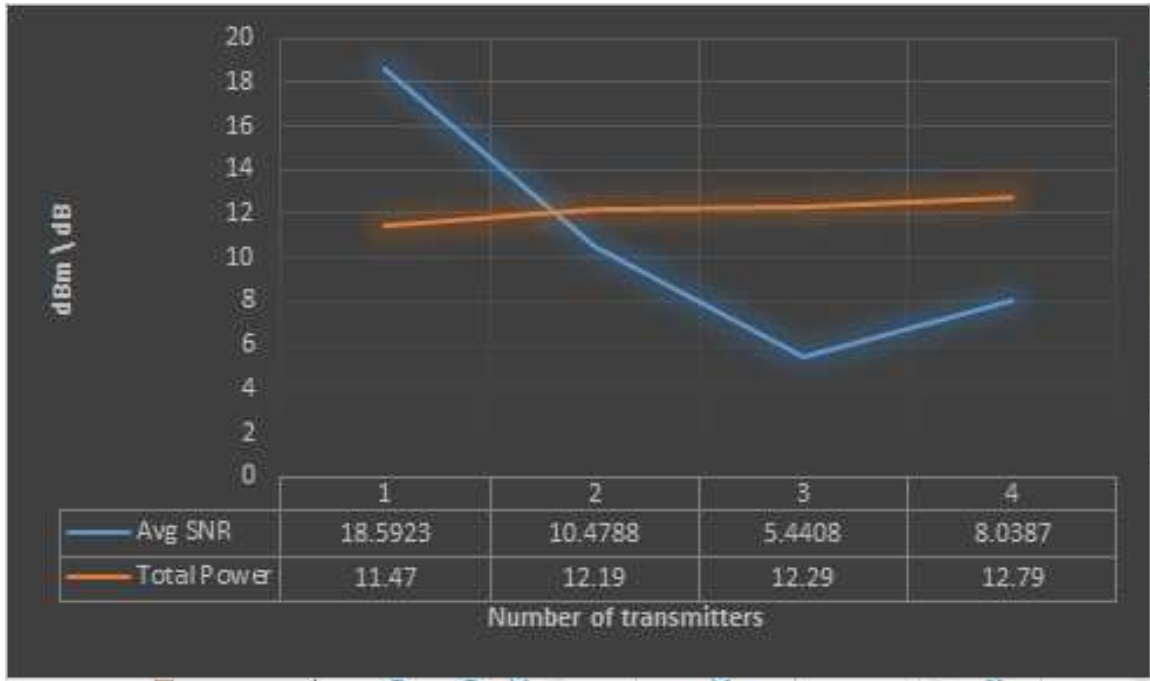


Figure 4.12: A graph showing how total transmit power and SINR change with increasing number of transmitters

is not the most efficient approach from a SINR perspective or equivalently from a capacity perspective.

#### 4.1.4 Exhaustive Enumeration

The method of Exhaustive enumeration (brute force) was chosen to be compared with our suggested algorithms. It is a simple discrete optimization technique. It first evaluates the optimum solution for all combinations of the discrete variables, then the best solution is obtained by scanning all the optimum solutions. It is a very time consuming algorithm. The time consumption depends greatly on the resolution of the discrete variables. It is important to note that if the resolution of the discrete variables was to tend to zero, exhaustive enumeration would provide exact results of the optimum. However, this can not be done since the time needed will tend, in this case, to infinity.

	Transmit Power	Transmitter Location
<b>Transmitter 1</b>	<b>8 dBm</b>	<b>D4-005-B (35)</b>
<b>Transmitter 2</b>	<b>8.5 dBm</b>	<b>D4-111-B (83)</b>
<b>Total secondary transmit power</b>	<b>11.2675 dBm</b>	

Figure 4.13: Results of exhaustive enumeration (brute force) method

Before using the different proposed approaches in simulations, it was crucial to have a benchmark that guides the evaluation process. Results of the exhaustive enumeration method is shown in Fig.4.13.

When comparing our approach to exhaustive enumeration, the power values provided by our algorithm are very accurate. While exhaustive enumeration results in a total secondary transmit power of 11.2675 dBm with very high time consumption, our algorithm results in a total secondary transmit power of 11.47 dBm which is 0.2 dB higher. It is important to note that if the resolution of the discrete variables in the exhaustive enumeration technique was to tend to zero, it would provide exact results of the optimum. However, this can not be done since the time needed will tend, in this case, to infinity.

The proposed algorithm takes less than 2 seconds to calculate the optimum position and power of 2 secondary transmitters. When compared to exhaustive enumeration, where the time consumption depends greatly on the accuracy required, it is safe to say that our algorithm is superior in both accuracy and time consumption. When the number of transmitters increases, the time needed for exhaustive enumeration increases exponentially reaching 5 days in the case of 4 transmitters with 0.2 dB resolution. However, the presented approach keeps an almost constant time consumption of 5 seconds at much higher accuracy. This is mainly achieved by keeping the algorithm time complexity the same for different number of transmitters. Since the

algorithm always depends on 2 nested loops, the time complexity doesn't change by increasing the number of transmitters  $K$ .

## 4.2 Approach 2 Results

In order to examine the validity of our approach for the optimization based on SINR, different simulations were done for different SINR thresholds. We limit our algorithm to only 2 possible secondary transmitters for the sake of simplicity and to avoid the computation complexity of having more than 2 secondary transmitters. However, this algorithm can be extended to explore  $K$  possible secondary transmitters but this is left for future works. As it is shown in Fig.4.14, different modulation schemes have different SINR requirements. We chose 4 different modulation schemes. 16 QAM 2/3, 16 QAM 3/4, 64 QAM 2/3 and 64 QAM 3/4. These modulation schemes correspond to SINR thresholds of 11.3, 12.2, 15.3 and 17.5 respectively [30]. We present the results in Fig.4.15.

From the results presented, it can be seen that different SINR requirements, like in the case of 64 QAM-3/4, result in a change in transmitter locations. The positions corresponding to indexes 5 and 82 are in different sides and floors of the building as shown in Fig.4.16. This is in-line with what was discussed in section 3.3 and what was presented in Fig.4.12. The clustering of transmitters in the same side of the building causes a drop in the average SINR value inside the building. It is important to note here that this algorithm optimizes only 2 different variables so far, transmitter locations and transmit powers. However, it can be extended to consider the number of transmitters. In this case, the number of transmitters plays a very important factor in the maximization of our QI.

Required Base Band SNR		
SNR Requirements Versus Coding Rate and Modulation Scheme		
Modulation	Code Rate	SNR [dB]
QPSK	1/8	-5.1
	1/5	-2.9
	1/4	-1.7
	1/3	-1.0
	1/2	2.0
	2/3	4.3
	3/4	5.5
	4/5	6.2
16 QAM	1/2	7.9
	2/3	11.3
	3/4	12.2
	4/5	12.8
64 QAM	2/3	15.3
	3/4	17.5
	4/5	18.6

Figure 4.14: A table showing different min SINR required for different modulation schemes [30]

Modulation Scheme	Min SINR required	Index of Tx 1 Position	Index of Tx 2 Position	Tx 1 transmit power	Tx 2 transmit power	QI percentage achieved (%)
16 QAM - 2/3	11.3 dB	35	83	7.5 dBm	7 dBm	98.79518072
16 QAM - 3/4	12.2 dB	35	83	7.5 dBm	7 dBm	98.79518072
64 QAM - 2/3	15.3 dB	35	83	7.5 dBm	7 dBm	95.18072289
64 QAM - 3/4	17.5 dB	5	82	2 dBm	0 dBm	78.31325301

Figure 4.15: A table showing results of maximizing the percentage of positions above a certain SINR threshold for different modulation schemes and their minimum SINR requirements

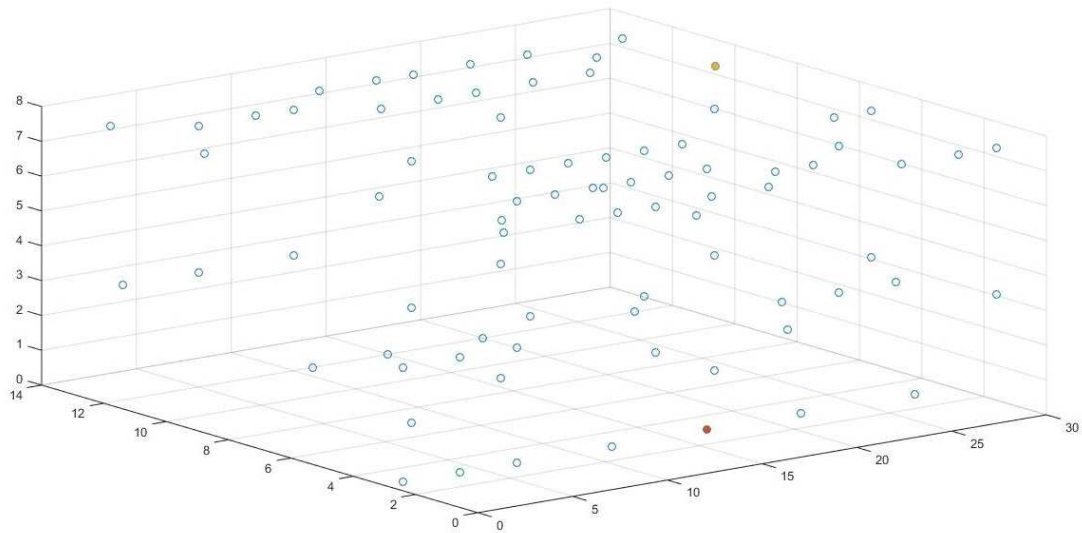


Figure 4.16: Positions of 2 secondary transmitters placed at index 5 and index 75 in fulfillment of high SINR requirements

## Chapter 5

### Conclusions and suggestions for future works

This thesis has proposed two different approaches to deploy indoor LTE secondary transmitters in the TVWS band assuming adjacent channel transmission. The objective was to introduce a model capable of optimizing secondary transmit powers and locations of secondary transmitters as well as find an optimum number of secondary transmitters for a given scenario.

First, an approach was proposed based on maximizing the total secondary transmit power. In the proposed approach, secondary transmit power and secondary transmitter locations are optimized. This approach had some convergence limitations that were handled by introducing a small modification to the algorithm that was proven to improve the consistency and the convergence rate of the algorithm. However, results have shown that maximizing the total secondary transmit power is accompanied by increasing the number of secondary transmitters which in some cases degrade the average SINR, hence the capacity of the system. Therefore, another approach was introduced based on maximizing the percentage of positions with SINR values higher than a desired SINR threshold. The scenario of having only two secondary transmitters was analyzed, and results were validated using extensive simulations in the considered building.

The proposed approach was compared to the brute force algorithm, also known as exhaustive enumeration algorithm, and it proved to be superior in time complexity



with mere seconds when considering high resolution (0.2 dB) in the results.

## 5.1 Suggestions for Future Works

Despite having not considered optimizing the number of transmitters in our approaches, the author believes that the two approaches can be extended to be able to optimize the number of transmitters. Future research will focus on the following points. First, proposing a more intelligent and time efficient algorithm for maximizing the percentage of positions with a SINR higher than a desired SINR threshold. This approach should be able to find exactly the optimum number of secondary transmitters, their transmit powers and their locations in order to maximize the network capacity inside the building. Second, in this thesis we only applied our approaches to the considered building. However, it is necessary to test the proposed model on different buildings, with already established REMs, and verify the generality of the two proposed algorithms. Third, the model should be tested on an interpolated version of the same REM (i.e where points with no real measurements are interpolated from nearby points with real measurements). In addition, we only considered, for our two approaches, maximizing the secondary transmit power and SINR. Other objectives should be considered that can better represent the coverage quality (i.e. capacity, Bit Error Rate (BER), etc.). Finally, secondary transmitters should be able to adapt to the changing capacity requirements within a building. This can be done by collecting statistical behavioral data about the users, integrating it into the REM, and proposing an approach that is dynamic enough to account for changing capacity needs in every part inside the building.

## Bibliography

- [1] Qualcomm, “Taking HSPA+ to the next level,” *Qualcomm.com*.
- [2] K. Harrison, S. Mishra, and A. Sahai, “How Much White-Space Capacity Is There?,” *New Frontiers in Dynamic Spectrum, 2010 IEEE Symposium on*, pp. 1–10, April 2010.
- [3] J. van de Beek, J. Riihijarvi, A. Achtzehn, and P. Mahonen, “TV White Space in Europe,” *Mobile Computing, IEEE Transactions on*, vol. 11, pp. 178–188, Feb 2012.
- [4] A. Umbert, J. Perez-Romero, F. Casadevall, A. Kliks, and P. Kryszkiewicz, “On the use of indoor Radio Environment Maps for HetNets deployment,” *Cognitive Radio Oriented Wireless Networks and Communications (CROWNCOM), 2014 9th International Conference on*, pp. 448–453, 2014.
- [5] A. Achtzehn, M. Petrova, and P. Mähönen, “Deployment of a Cellular Network in the TVWS: A Case Study in a Challenging Environment,” *Proceedings of the 3rd ACM Workshop on Cognitive Radio Networks*, pp. 7–12, 2011.
- [6] H. Bogucka and J. Perez-Romero, “Small cells deployment in TV White Spaces with neighborhood cooperation,” *General Assembly and Scientific Symposium (URSI GASS), 2014 XXXIth URSI*, pp. 1–4, Aug 2014.
- [7] A. Achtzehn, M. Petrova, and P. Mahonen, “On the performance of cellular network deployments in TV white spaces,” *Communications (ICC), 2012 IEEE International Conference on*, pp. 1789–1794, June 2012.
- [8] J. Mitola and J. Maguire, G.Q., “Cognitive radio: making software radios more personal,” *Personal Communications, IEEE*, vol. 6, pp. 13–18, Aug 1999.
- [9] J. Xiao, R. Hu, Y. Qian, L. Gong, and B. Wang, “Expanding LTE network spectrum with cognitive radios: From concept to implementation,” *Wireless Communications, IEEE*, vol. 20, pp. 12–19, April 2013.
- [10] I. F. Akyildiz, W.-Y. Lee, M. C. Vuran, and S. Mohanty, “Next generation/dynamic spectrum access/cognitive radio wireless networks: A survey,” *Comput. Netw.*, vol. 50, pp. 2127–2159, Sept. 2006.
- [11] A. BRYDON, “UK moves towards dynamic access for TV white space spectrum,” *Unwired Insight*, Sep 2013.

- [12] J. Mwangoka, P. Marques, and J. Rodriguez, "Exploiting tv white spaces in europe: The cogeu approach," *New Frontiers in Dynamic Spectrum Access Networks (DySPAN)*, 2011 IEEE Symposium on, pp. 608–612, May 2011.
- [13] C. F. Silva, H. Alices, and A. Gomes, "Extension of lte operational mode over tv white spaces," *Proc. of Future Network and Mobile Summit*, 2011.
- [14] J. Markendahl, P. Gonzalez-Sanchez, and B. Molleryd, "Impact of deployment costs and spectrum prices on the business viability of mobile broadband using TV white space," *Cognitive Radio Oriented Wireless Networks and Communications (CROWNCOM)*, 2012 7th International ICST Conference on, pp. 124–128, June 2012.
- [15] Z. Zhao, M. Schellmann, H. Boulaaba, and E. Schulz, "Interference study for cognitive LTE-femtocell in TV white spaces," *Telecom World (ITU WT)*, 2011 Technical Symposium at ITU, pp. 153–158, Oct 2011.
- [16] A. Kliks, P. Kryszkiewicz, A. Umbert, J. Perez-Romero, and F. Casadevall, "TVWS Indoor measurements for HetNets," *Wireless Communications and Networking Conference Workshops (WCNCW)*, 2014 IEEE, pp. 76–81, 2014.
- [17] H. Liang, B. Wang, W. Liu, and H. Xu, "A Novel Transmitter Placement Scheme Based on Hierarchical Simplex Search for Indoor Wireless Coverage Optimization," *Antennas and Propagation, IEEE Transactions on*, vol. 60, pp. 3921–3932, Aug 2012.
- [18] L. Mohjazi, M. Al-Qutayri, H. Barada, and K. Poon, "Femtocell coverage optimization using genetic algorithm," *Telecom World (ITU WT)*, 2011 Technical Symposium at ITU, pp. 159–164, Oct 2011.
- [19] L. Ho, I. Ashraf, and H. Claussen, "Evolving femtocell coverage optimization algorithms using genetic programming," *Personal, Indoor and Mobile Radio Communications, 2009 IEEE 20th International Symposium on*, pp. 2132–2136, Sept 2009.
- [20] A. Dalla'Rosa, A. Raizer, and L. Pichon, "Comparative study between kriging and genetic algorithms for optimal transmitter location in an indoor environment using transmission line modeling," *Computational Electromagnetics (CEM)*, 2006 6th International Conference on, pp. 1–2, April 2006.
- [21] A. Dalla'Rosa, A. Raizer, and L. Pichon, "Optimal indoor transmitters location using tlm and kriging methods," *Magnetics, IEEE Transactions on*, vol. 44, pp. 1354–1357, June 2008.
- [22] S. Valizadeh and J. Abouei, "An adaptive distributed coverage optimization scheme in lte enterprise femtocells," *Electrical Engineering (ICEE)*, 2014 22nd Iranian Conference on, pp. 1723–1728, May 2014.

- [23] Y. Zhao, J. Reed, S. Mao, and K. K. Bae, "Overhead analysis for radio environment map-enabled cognitive radio networks," *Networking Technologies for Software Defined Radio Networks, 2006. SDR '06.1st IEEE Workshop on*, pp. 18–25, Sept 2006.
- [24] A. T. S. Committee, "ATSC Recommended Practice: Receiver Performance Guidelines (with Corrigendum No. 1 and Amendment No.1)," *Doc. A/74*, November 2007.
- [25] H. Aiache and e. al., "Use-cases Analysis and TVWS Systems Requirements," *Deliverable D3.1 of the COGEU project*, August 2010.
- [26] G. Stuber, S. Almalfouh, and D. Sale, "Interference analysis of tv-band whitespace," *Proceedings of the IEEE*, vol. 97, pp. 741–754, April 2009.
- [27] Alcatel-Lucent, "Simulation assumptions and parameters for fdd hennb rf requirements," *3GPP TSG RAN WG4 Meeting 51: R4-092042*, May 2009.
- [28] J. Lauterjung and et al., "Spectrum measurements and anti-interference spectrum database specification," *Deliverable D4.1 of the COGEU project*, October 2010.
- [29] S. Hohmann, "Optimization of Dynamic Systems Lecture notes," *Institute of Control Systems*, October 2013.
- [30] Rhode and Schwarz, "Lte: System specifications and their impact on rf and base band circuits," *Application Notes*.
- [31] J. Kwak and A. Demir, "Signal to Noise+Interference (SNIR) Variations on multiple TVWS channels," *IEEE*, July 2012.
- [32] V. Hlaváč, K. Jeffery, and J. Wiedermann, "Exhaustive search, combinatorial optimization and enumeration: Exploring the potential of raw computing power," *SOFSEM 2000: Theory and Practice of Informatics*, vol. 1963, 2000.